



Article

Predictive Potential of Maize Yield in the Mesoregions of Northeast Brazil

Fabrício Daniel dos Santos Silva ¹, Ivens Coelho Peixoto ¹, Rafaela Lisboa Costa ¹, Helber Barros Gomes ¹, Heliofábio Barros Gomes ¹, Jório Bezerra Cabral Júnior ², Rodrigo Martins de Araújo ¹ and Dirceu Luís Herdies ^{3,*}

¹ Institute of Atmospheric Sciences, Federal University of Alagoas, Maceió 57072-900, Brazil; fabricio.santos@icat.ufal.br (F.D.d.S.S.); ivenspeixoto@hotmail.com (I.C.P.); rafaela.costa@icat.ufal.br (R.L.C.); helber.gomes@icat.ufal.br (H.B.G.); heliofabio@icat.ufal.br (H.B.G.); rmatematica@hotmail.com (R.M.d.A.)

² Institute of Geography, Development and Environment, Federal University of Alagoas, Maceió 57072-900, Brazil; jorio.cabral@igdema.ufal.br

³ National Institute for Space Research, Cachoeira Paulista, São Paulo 12630-000, Brazil

* Correspondence: dirceu.herdies@inpe.br

Abstract: Most of the northeastern region of Brazil (NEB) has a maize production system based on family farming, with no technological advances and totally dependent on the natural rainfall regime, which is concentrated in 4 to 5 months in most parts of the region. This means that the productivity of this crop is low in the NEB. In the northern mesoregions of the NEB, rainfall is concentrated between January and June, in the east of the NEB from April to September, and in the west of the NEB from October to March. The growing season takes place during these semesters. With this in mind, our objective was to develop a model based on canonical correlation analysis (CCA) to predict corn production in the mesoregions of the NEB between 1981 and 2010, using accumulated precipitation per semester as the predictor variable and predicting the observed production in kg/ha. Our results showed that the CCA model presented higher correlations between observed and simulated production than that obtained simply from the direct relationship between accumulated rainfall and production. The other two metrics used, *RMSE* and *NRMSE*, showed that, on average, in most mesoregions, the simulation error was around 200 kg/ha, but the accuracy was predominantly moderate, around 29% in most mesoregions, with values below 20% in six mesoregions, indicative of better model accuracy, and above 50% in two mesoregions, indicative of low accuracy. In addition, we investigated how the different combinations between two modes of climate variability with a direct influence on precipitation in the NEB impacted production in these 30 years, with the combination of El Niño and a positive Atlantic dipole being the most damaging to harvests, while years when La Niña and a negative Atlantic dipole acted together were the most favorable. Despite the satisfactory results and the practical applicability of the model developed, it should be noted that the use of only one predictor, rainfall, is a limiting factor for better model simulations since other meteorological variables and non-climatic factors have a significant impact on crops. However, the simplicity of the model and the promising results could help agricultural managers make decisions in all the states that make up the NEB.

Keywords: Northeast Brazil; maize yield; canonical correlation analysis



Citation: Silva, F.D.d.S.; Peixoto, I.C.; Costa, R.L.; Gomes, H.B.; Gomes, H.B.; Cabral Júnior, J.B.; de Araújo, R.M.; Herdies, D.L. Predictive Potential of Maize Yield in the Mesoregions of Northeast Brazil. *AgriEngineering* **2024**, *6*, 881–907. <https://doi.org/10.3390/agriengineering6020051>

Academic Editor: Murali Krishna Gumma

Received: 5 February 2024

Revised: 15 March 2024

Accepted: 25 March 2024

Published: 2 April 2024



Copyright: © 2024 by the authors. Licensee MDPI, Basel, Switzerland. This article is an open access article distributed under the terms and conditions of the Creative Commons Attribution (CC BY) license (<https://creativecommons.org/licenses/by/4.0/>).

1. Introduction

Every year, Brazil consolidates its position as one of the world's leading grain producers, especially of soybeans and maize. According to CONAB (the national supply company responsible for monitoring and estimating Brazilian agricultural production), the grain harvest for the 2019/2020 season was 102.3 million tons [1], while for the 2023/2024 harvest, the estimate is 312.3 million tons of grain [2]. These figures show the average annual evolution of Brazilian grain production.

Maize stands out in this production scenario, giving Brazil third place in the world in the production of this grain, with approximately 12% of world production, behind only the United States (30% of world production) and China (24% of world production). Maize is essential in the production of biofuels [3], as well as being the staple food for billions of people around the world. It contains vitamins A and B, proteins, fats, carbohydrates, calcium, iron, phosphorus, and starch [4]. In Brazil, this cereal is also the main component used in the production of animal supplementation, destined for one of the main segments of Brazilian exports, which is the animal protein production chain [5,6].

Despite the high productivity of some Brazilian regions and their prominent role in world maize production, in the Northeast of Brazil (NEB), most mesoregions still grow maize through subsistence farming, with little or no mechanization and low technological potential. According to Garnett and Khandekar [7], the socio-economic impact on production is more intense in areas where there are major changes in climatic conditions, so it is understood that production varies considerably from year to year, which is the case in the NEB [8].

Water is a crucial factor in the development of the maize plant, the deficit of which is one of the main causes of a drop in productivity [9]. The need for water, temperature, and solar radiation are variables that directly affect the growth period, which reaches its maximum when these variables are optimally available, making it easier for the crop to reach its maximum yield capacity. In tropical conditions, according to the smaller variation in temperature and day length, the distribution of rainfall generally determines the best sowing time [10].

Maize consumes, on average, 400 to 700 mm of water in its complete cycle, depending on climatic conditions. Its period of maximum water demand occurs during the formation and filling of grains, that being the period in which water deficit causes the greatest reduction in its productivity [9]. Temperature is the main regulator of maize phenology, determining the emergence of seedlings and the rate of appearance of new leaves. Furthermore, the ideal soil temperature during the germination period is between 25 °C and 30 °C, with temperatures below 10 °C and above 40 °C being harmful to germination. Knowing that the ideal average environmental temperature for emergence and flowering is between 24 °C and 30 °C [11–14], in terms of this variable, the NEB as a whole contemplates the crop's thermal needs, since its average annual temperature varies between 20 °C and 28 °C, with a variation from 24 °C to 26 °C in areas located above 200 m of altitude, and below 20 °C in elevated areas of *Chapada Diamantina* and *Planalto da Borborema* [15,16].

In the NEB, the high interannual variability of rainfall, climatically concentrated in a few months and marked by spatio-temporal variation, makes farming a high-risk activity, often doomed to total crop losses or low productivity [17]. Climate change scenarios for the region, with a decrease in accumulated rainfall and an increase in evapotranspiration, inspire even more concern for future yields [18]. Between 2012 and 2018, the NEB went through one of its longest droughts, both in terms of duration, magnitude, and intensity [19–23]. Medeiros et al. [24] showed that indices of climatic extremes indicate a reduction in rainfall in much of the Northeast in recent decades, and Pontes Filho et al. [25] showed that all areas of the NEB are highly susceptible to the return of droughts on different scales.

In regions, like the NEB, which are directly dependent on rainfall variability, the intensity of the loss associated with the harvest is greater, the greater is the shortage of rainfall. In this way, a useful tool for decision-making processes in agriculture would be a good crop forecast based on a prediction of the accumulated rainfall during the crop's growing season. In this sense, the innovative nature of this research is to analyze the predictive potential of maize crop productivity in all the mesoregions of the NEB through the relationship between historical productivity and accumulated rainfall in the rainy semester, using the multivariate analysis technique Canonical Correlation Analysis (CCA). With this, we sought to correlate and identify the periods of greatest influence of rainfall on maize productivity in the mesoregions of the NEB, calibrate a crop forecasting model based on CCA, and also quantify the influence of the two main modes of climate variability that

affect the distribution of rainfall in the mesoregions of the NEB, ENOS and the Atlantic dipole, and their respective impacts on maize productivity.

2. Materials and Methods

2.1. Data and Area of Study

The NEB is located between latitudes 1° and 21° S, and between longitudes 32° and 49° W, occupying around 18% of the Brazilian territory with 1.6×10^6 km² [26], divided into nine states: Maranhão (MA), Piauí (PI), Ceará (CE), Rio Grande do Norte (RN), Paraíba (PB), Pernambuco (PE), Alagoas (AL), Sergipe (SE) and Bahia (BA). These nine states are subdivided into 42 mesoregions, as shown in Figure 1. For each mesoregion, the wettest semester was identified. This task, simple but essential to the research, was carried out to simulate maize productivity in each mesoregion considering an average cycle of 120 days for the crop, so as not to risk making the mistake of not adjusting the rainy season to the planting period. As an example, for a given mesoregion where the wettest semester is January to June, the entire crop cycle, of four months on average, would fall within it. Table 1 shows the wettest semester in each mesoregion.

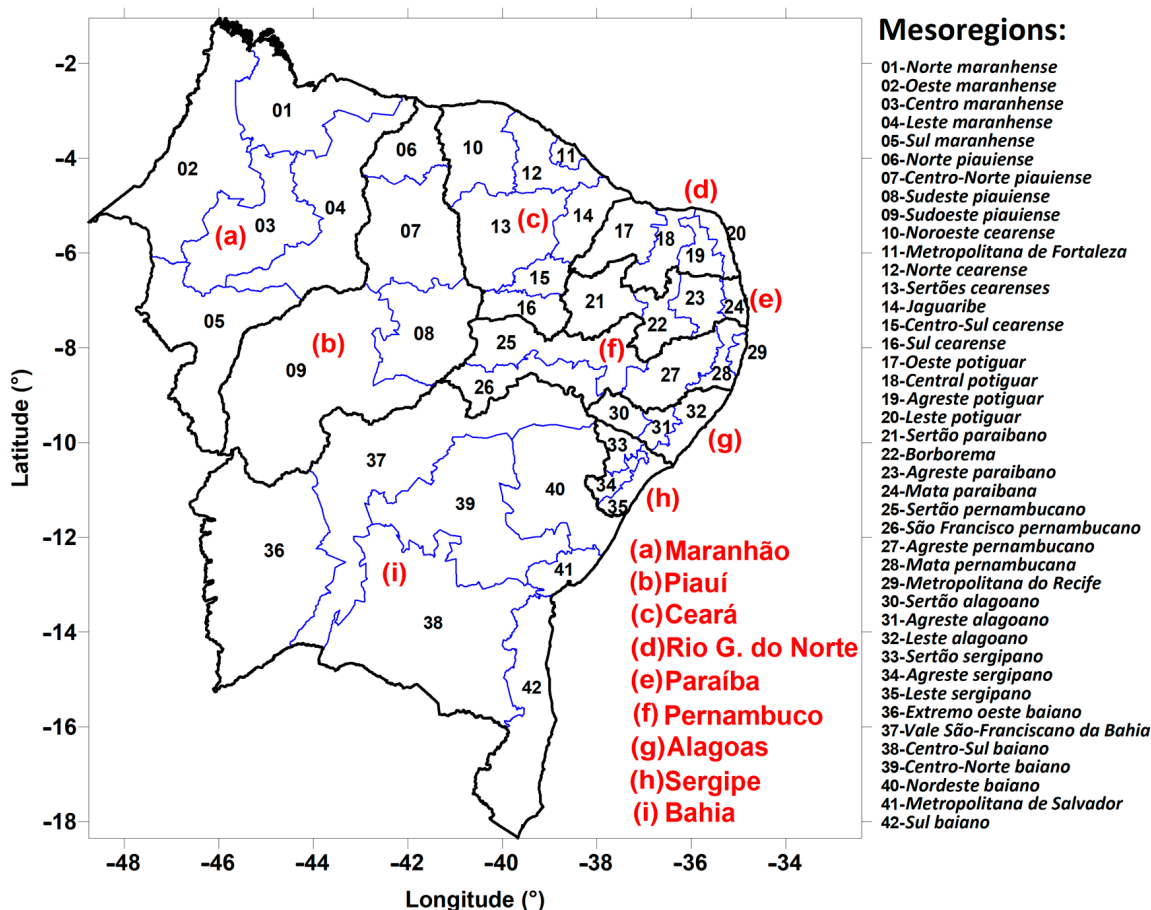


Figure 1. Map of the Northeast region of Brazil identifying the nine states, (a) Maranhão, (b) Piauí, (c) Ceará, (d) Rio Grande do Norte, (e) Paraíba, (f) Pernambuco, (g) Alagoas, (h) Sergipe and (i) Bahia, and identifying the 42 mesoregions, numbered between the states.

We used the monthly rainfall time series from 97 weather stations of the National Institute of Meteorology (INMET), from 1961 to the present, whose data underwent the quality control and gap filling described in [27]. The location of the stations can be seen in Figure 2a, while Figure 2b shows the distribution of the mesoregions by rainy semester.

Table 1. Mesoregions of the NEB and respective rainy semester.

| Mesoregion | Rainy Season |
|--|--------------------------------|
| <i>Norte maranhense</i> <i>Oeste maranhense</i> <i>Central maranhense</i> <i>Leste maranhense</i> <i>Norte piauiense</i> <i>Centro Norte piauiense</i> <i>Sudeste piauiense</i> <i>Noroeste cearense</i> <i>Metropolitana de Fortaleza</i> <i>Norte cearense</i> <i>Sertões cearenses</i> <i>Jaguaribe</i> <i>Centro-Sul cearense</i> <i>Sul cearense</i> <i>Oeste potiguar</i> <i>Central potiguar</i> <i>Sertão paraibano</i> <i>Borborema</i> <i>Sertão pernambucano</i> <i>São-Francisco pernambucano</i> <i>Vale São Franciscano da Bahia</i> <i>Centro-Norte baiano</i> | January to June (JFMAMJ) |
| <i>Sul maranhense</i> <i>Sudoeste piauiense</i> <i>Extremo oeste baiano</i> <i>Centro-Sul baiano</i> | October to March (ONDJFM) |
| <i>Agrete potiguar</i> <i>Leste potiguar</i> <i>Agrete paraibano</i> <i>Mata paraibana</i> <i>Agrete pernambucano</i> <i>Mata pernambucana</i> <i>Metropolitana do Recife</i> <i>Sertão alagoano</i> <i>Agrete alagoano</i> <i>Leste alagoano</i> <i>Sertão sergipano</i> <i>Agrete sergipano</i> <i>Leste sergipano</i> <i>Sul baiano</i> <i>Nordeste baiano</i> <i>Metropolitana de Salvador</i> | April to September (AMJJAS) |

The yield data were collected from the Statistical Database of the Automatic Retrieval System (SIDRA) of the Brazilian Institute of Geography and Statistics (IBGE), for the period from 1974 to 2018. However, the rainfall and yield database was worked on for a common period to eliminate continuity problems observed at the beginning of the maize yield series for each mesoregion, homogenizing them without the need to fill in gaps. The common period of data was from 1981 to 2010, 30 years, the same period used to generate the rainfall climatology for each mesoregion and identify the wettest semesters.

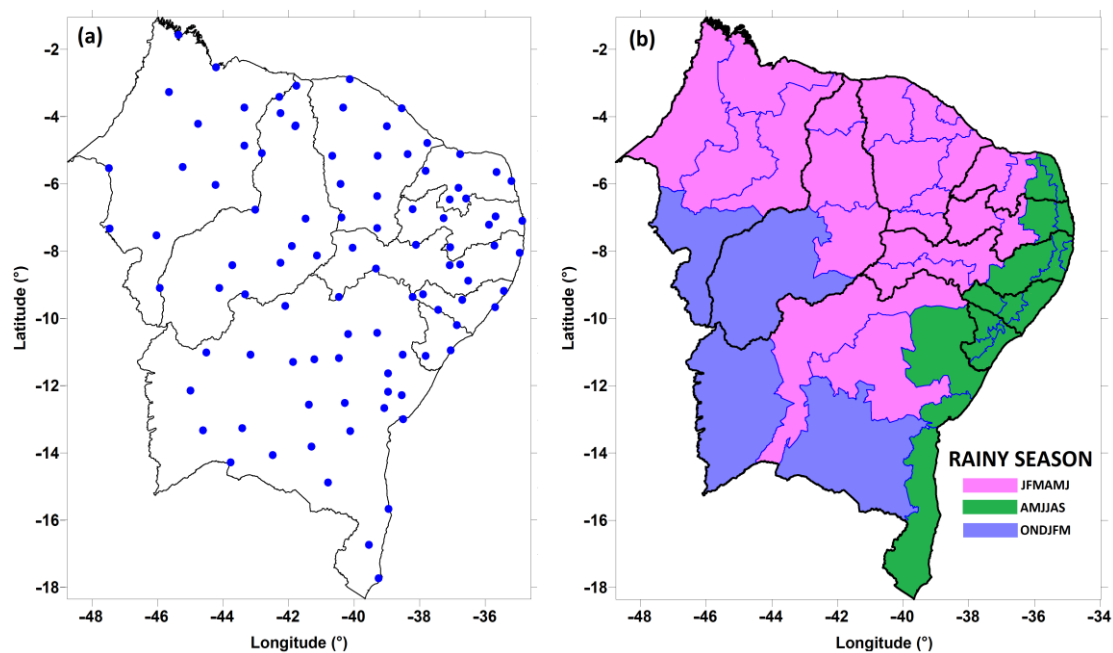


Figure 2. (a) Geographical distribution of the 97 conventional weather stations in the NEB states; (b) rainy semester for each NEB mesoregion.

2.2. Canonical Correlation Analysis

CCA is a multivariate analysis technique widely used to generate operational climate forecasts [28–30]. It can be used in two ways (see Figure 1 of [31]): the first by relating raw outputs from dynamic models to observations—for example, relating predicted cumulative precipitation of a month/quarter relative to a past reference period (hindcast) with the actual observations of that period, and thus recalibrate and correct biases in these predictions, allowing this correction to be applied to future model predictions; the second way, and the method used in this research, is to build a purely statistical forecasting model, relating a predictor to a predictand; in our case, observed precipitation fields with maize production data in mesoregions of the NEB. This methodology is like seasonal forecasting with CCA, relating TSM (predictor) to precipitation (predictand).

Precipitation totals for the JFMAMJ, AMJJAS, and ONDJFM semesters were the predictors (X), and the average maize yield for each NEB mesoregion was the predictand (Y). Both fields are pre-filtered with Empirical Orthogonal Functions (EOF) to eliminate noise from the original data [32]. In this process, the EOFs of X and Y are calculated separately, establishing a model that retains around 70% to 80% of the original variance of each variable from several eigenvectors. This process forces the CCA to emphasize the dominant modes of variability of X and Y. Next, a cross-correlation matrix is constructed with the series of principal components of X and Y, whose dimensions are reduced to the number of modes retained by the predictor and the predictand, obtaining canonical eigenvectors and eigenvalues for X and Y from this transposed matrix.

The canonical function of the predictor is found from the linear combinations between the canonical eigenvectors and the series of principal components of the predictor for each mode. Although a limited number of modes can be used based on the analysis of variance explanation, it is recommended to set a minimum of 1 mode to a maximum of 10 modes as limits in the script developed in R software, version 4.0.3 (<https://www.r-project.org/> (accessed on 5 August 2023)). This is recommended because it allows the software to automatically find the optimum number of modes based on a model goodness index, which adjusts the number of modes according to the correlation obtained from testing various models with different combinations of modes for X and Y, which generally limits the number of modes to between 3 and 6, respectively. The regression equation expressed

by the canonical modes is derived from the original variables by converting the canonical temporal function of the predictor into the canonical temporal function of the predictand.

Finally, the predictive equation is obtained to relate the predictor to the predictand, or X to Y, and historical simulations and/or forecasts can be carried out. This research was limited to historical simulations, and it is recommended for subsequent research to test the model for forecasts based on outputs from models such as the NMME family [33] and ECMWF [34]. Figure 3 provides a schematic illustration of the steps required to simulate production (predictand Y) as a function of the six-month accumulated rainfall fields (predictor X).

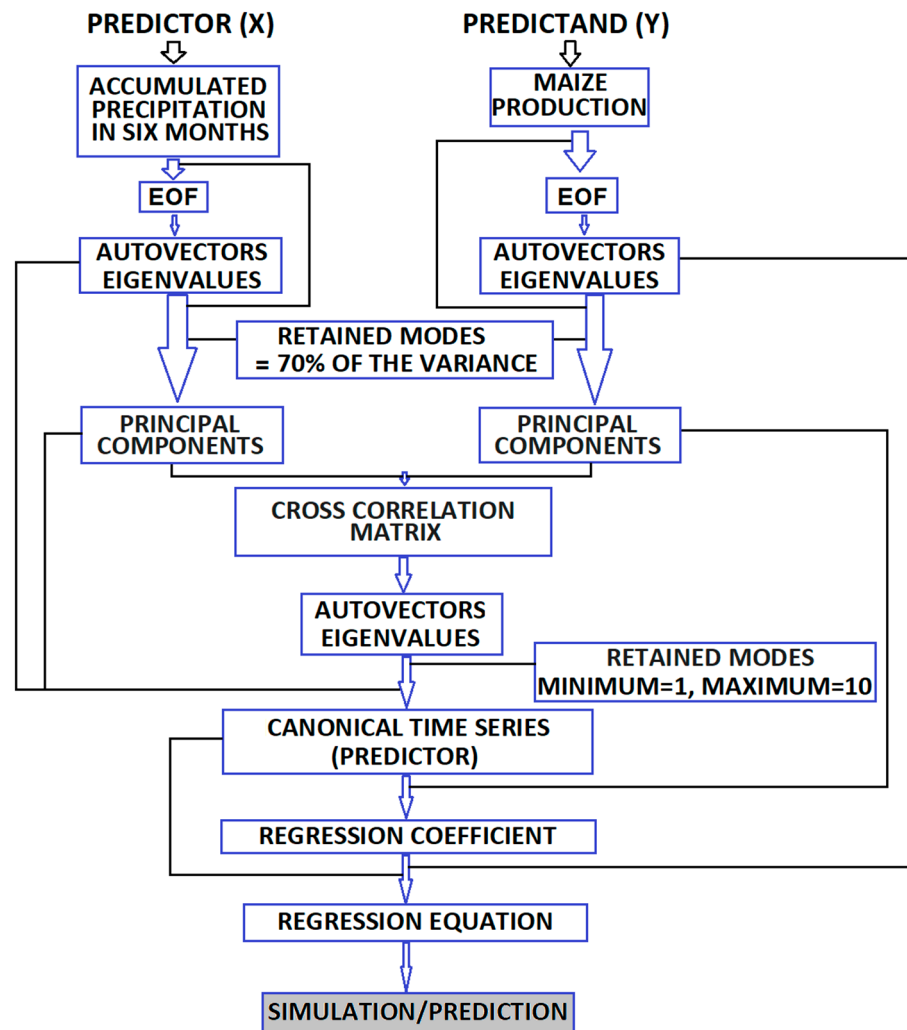


Figure 3. Illustrative diagram of the steps used to simulate maize production in the NEB mesoregions based on semi-annual accumulated precipitation, using CCA.

To assess the relationship between accumulated rainfall and maize yield, before and after the application of CCA, we used Pearson’s correlation coefficient (r), given by Equation (1), which serves to measure the strength of the linear relationship between sets of data. We used the parametric Student’s t -test to verify the statistical significance of the correlations at a 95% confidence interval (p -value < 0.05), which according to the sample size, indicates a critical correlation coefficient of approximately 0.4, a value for which the statistical hypothesis that there is a correlation between the data sets can be accepted, in this case, between the cumulative six-month rainfall and maize production in each mesoregion of the NEB.

The other metrics used to evaluate the model were the root-mean-square error ($RMSE$) and the normalized root-mean-square error ($NRMSE$). The main advantage of the $RMSE$ is

that it penalizes errors of greater magnitude, in the same unit as the variable of interest, in our case, the production in kg/ha simulated in each mesoregion by the CCA model. Therefore, the greater the difference between simulations and observations, the greater the *RMSE* values [27]. However, the accuracy of the model is not well assessed with the *RMSE*, and it is necessary to assess it objectively. To fulfill this function, the *NRMSE* is a metric indicated by showing in percentage terms how much the model tends to estimate values that are closer or further away from the observation. The *RMSE* can be normalized by the mean of the observations, by the difference between the maximum and minimum values observed, by the standard deviation of the observation, and even by the interquartile range. In our case, we obtained the *NRMSE* by normalizing the *RMSE* with the mean of the observations, due to the high interannual variability of the observations over the 30 years analyzed. In general, *NRMSE* values < 20% indicate good model performance. The *RMSE* and *NRMSE* are obtained according to Equations (1) and (2) below.

$$RMSE_{(s,o)} = \sqrt{\frac{1}{n} \sum_{i=1}^n (s_i - o_i)^2} \quad (1)$$

$$NRMSE = \frac{RMSE}{\mu} \quad (2)$$

where n is the total number of elements in the series, s_i = simulated value (s) by the model in each year i , o_i = observed production in each year i , and μ is the average of the observations.

3. Results and Discussion

3.1. Relation between Rainfall and Production

Figure 4 shows the average accumulated rainfall in the wettest semester for each NEB mesoregion (Figure 4a), the average production for each mesoregion (Figure 4b), and the direct correlation between rainfall data and production in the 1981–2010 period (Figure 4c). Figure 4a shows that the highest accumulated rainfall is observed in all the mesoregions of the state of Maranhão, in the *Norte* and *Centro-Norte* mesoregions of Piauí, and in mesoregions of the eastern band of the NEB, between the states of Rio Grande do Norte and Bahia, with values that exceed, on average, 1000 mm of accumulated rainfall, with the maximum observed in the mesoregion *Norte maranhense*, at 1960 mm. In contrast, the lowest accumulated rainfall values occur in mesoregions of the central portion of the NEB, from Ceará to Bahia, with the lowest values belonging to the *São Francisco* and *Agreste* mesoregions in Pernambuco (407 mm and 458 mm), and in the *Vale São-Franciscano*, *Centro-Norte* and *Nordeste* mesoregions in Bahia (405 mm, 413 mm and 441 mm).

Figure 4b shows that the highest yields are concentrated in the *Sul maranhense*, *Sudoeste piauiense* and *Extremo oeste baiano* mesoregions (1710 kg/ha, 825 kg/ha, and 2158 kg/ha, respectively), within the region known as MATOPIBA, where cheap land prices, climate, and topography are favorable to extensive rainfed agriculture [35]. In most of the other central mesoregions of the NEB, the semi-arid climate makes them extremely vulnerable to adversities such as droughts, which are recurrent, raising the risks of loss of income for small farmers who depend on growing crops that are not well adapted to droughts, such as maize, whose production is generally less than 800 kg/ha, or less than a fifth of the average yield in other Brazilian regions [26].

The correlation (r) between accumulated rainfall in the wettest semester and observed production in the 1981–2010 period is shown in Figure 4c. Many mesoregions show r values of less than 0.4, i.e., without statistical significance according to the Student's t -test used. However, for other mesoregions the correlation exceeds this value, showing that there is a significant relationship between accumulated rainfall in the growing season (wettest semester) and production. However, this relationship is not enough to reliably predict production values, especially in series that have some kind of trend, and it is necessary to apply some method that allows accumulated rainfall to be used as input data for predicting production.

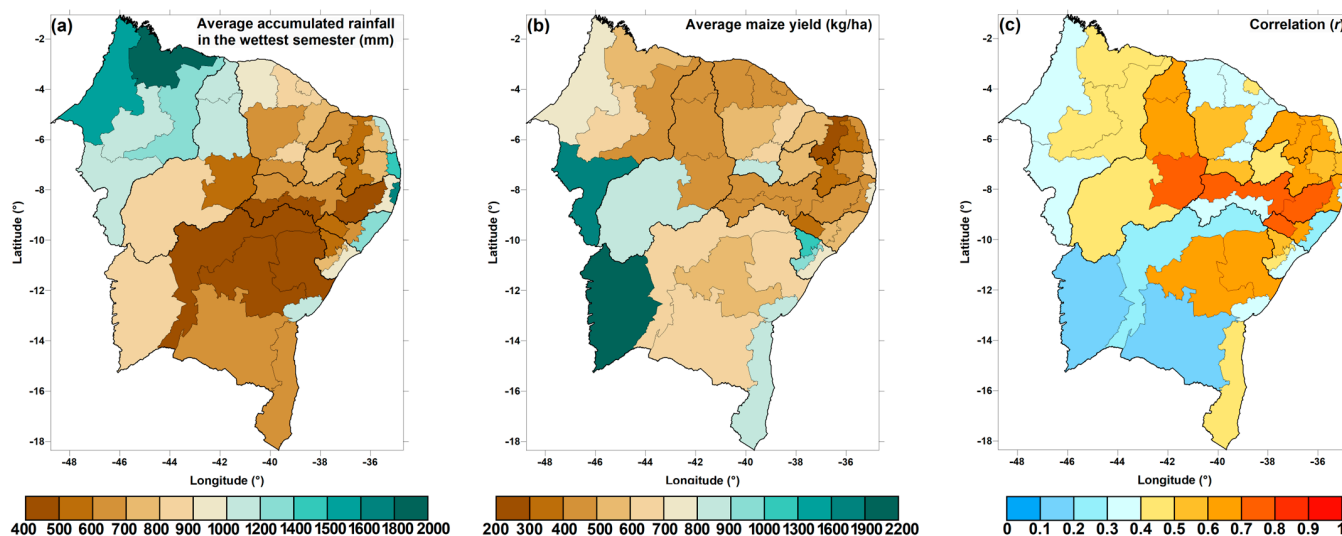


Figure 4. (a) Average rainfall for the wettest semester in each NEB mesoregion, in millimeters, (b) average maize production in kg/ha, and (c) correlation between accumulated rainfall in the growing season in each mesoregion and observed production. For the sample size of 30 years, all correlations above 0.4 are statistically significant according to the Student’s *t*-test. Obtained for the period 1981–2010.

3.2. Results Obtained by the CCA Model

After checking the wettest semester in each mesoregion, shown in Figure 2, the CCA model was designed to operate with 1 to 10 modes of variability, following the flowchart shown in Figure 5. The explanatory variable, or predictor (X), was the accumulated rainfall, considering the wettest semester in each mesoregion and in which, according to the CONAB agricultural calendar, maize is grown. For each mesoregion, the variable to be explained, or predicted (Y), was obtained, which was the average production in kg/ha of the mesoregion obtained from IBGE. The model was built for 30 years from 1981 to 2010.

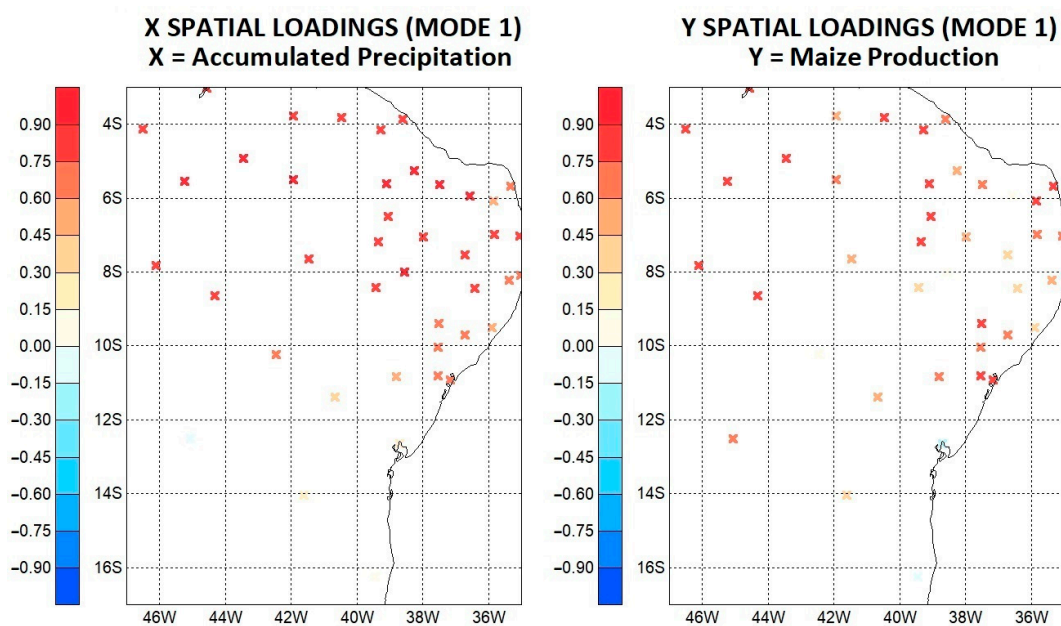


Figure 5. Spatial loads of X and Y (mode 1) show the most dominant pattern in the correlation of rainfall associated with above-normal production. The canonical correlation for this pair of variables was over 0.92. From the time points (mode 1), rainfall patterns, above or below normal, tend to coincide with above-normal production and vice versa. They were obtained for the period 1981–2010.

Figure 5 shows, for the centroid of each NEB mesoregion, the spatial loadings of the first mode of variability for predictor X and predictor Y. The first mode is the most dominant in the correlation between accumulated rainfall and production, showing that canonical loads associated with above-average rainfall are associated with above-average production. The canonical correlation for this pair of variables was 0.92 for the first mode, which explains more than 50% of the variance in the production data, directly proportional, as indicated in Figure 6. According to [36], retained modes of variability that explain more than 70% of the variance in the data are sufficient for building a predictive statistical model, since other modes can only add noise to the model without necessarily improving the predicted values.

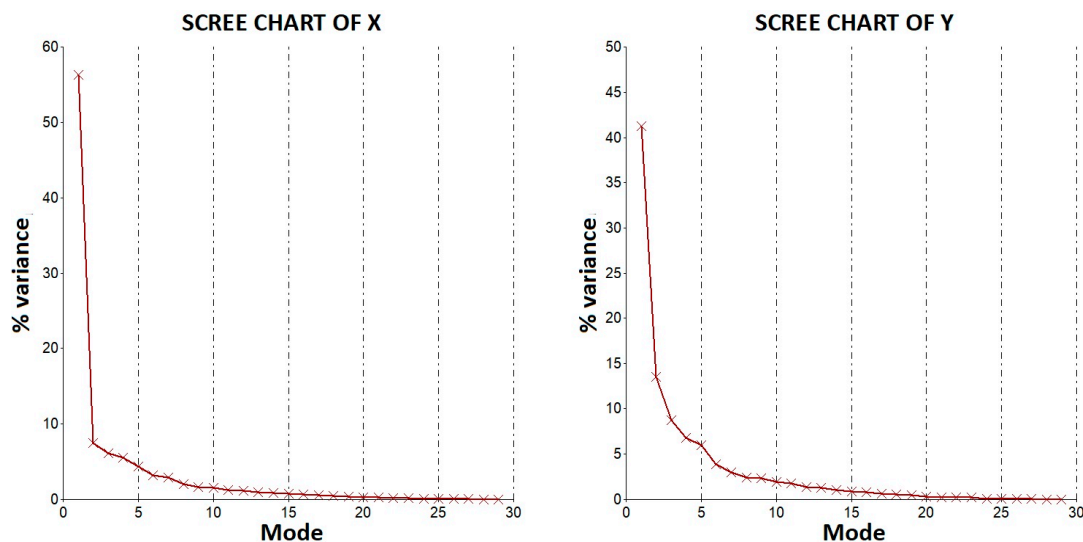


Figure 6. Scree plot of the number of modes retained in the principal component analysis.

In simpler terms, the association between the rainfall in the wettest half of the year and the production observed in each mesoregion is defined by the linear combination of the index values associated with each of the sets (EOFs), maximizing the correlation between the two indices and retaining as much information as possible contained in the original variables. Figure 5 shows scree plots for X and Y. The scree plot in multivariate statistics shows the line of factors or principal components of the analysis and is used to determine the number of factors retained or principal components maintained in an analysis, in this case, CCA. Figure 6 shows that for X, the first five factors explain 83% of the variance, and these were chosen to build the prediction model (57% for the first mode or principal component, 8% for the second mode, 7% for the third mode, 6% for the fourth mode and 5% for the fifth mode). The correspondence in Y for the first five modes is consistent with the X modes, only with percentages of explanation of the variance of the production data slightly below those observed in the X modes (accumulated rainfall).

Interpreting the *RMSE* as the average deviation of the forecasts from the observations, Figure 7a shows a strong predominance of deviations of less than 300 kg in most mesoregions, with seven of them having values of less than 100 kg/ha, in the *Norte maranhense*, *Noroeste cearense*, *Agreste* and *Mata pernambucana*, *Sertão* and *Leste alagoano*, and *Sul baiano*. The exception is the mesoregions of *Sul maranhense* and *Extremo oeste baiano*, with *RMSE* values of more than 800 kg/ha. This is because these mesoregions belong to the MATOPIBA area, whose agricultural activity is different from the others, being practiced extensively with a clear tendency for productivity to increase from the 2000s onwards. This upward trend in production throughout the series makes it difficult to simulate the model, which is unable to follow this behavior accurately, resulting in strong differences between the predicted and observed values, thus increasing the forecast errors, which are naturally reflected in the high *RMSE* values.

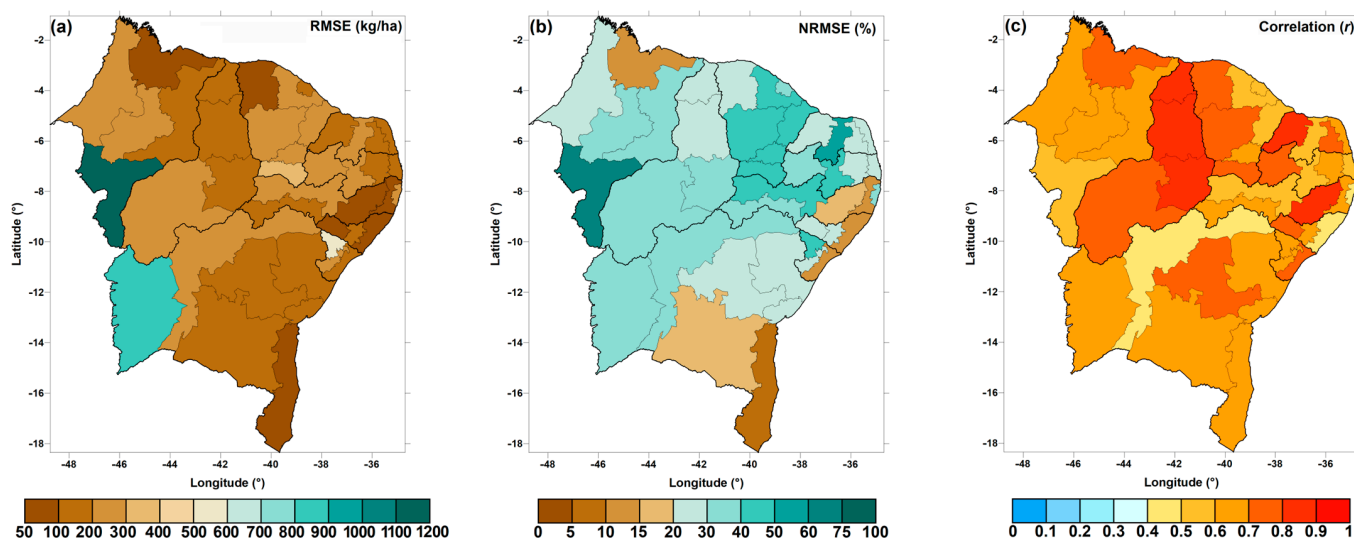


Figure 7. (a) RMSE in kg/ha between observed and simulated production, (b) NRMSE in % between observed and simulated production, and (c) correlation between observed and simulated production with CCA. For the sample size of 30 years, all correlations above 0.4 are statistically significant according to the Student's *t*-test. Obtained for the period 1981–2010.

Taking as a reference that *NRMSE* values < 20% indicate good model performance, it can be seen that the model was highly accurate in the historical simulation of corn production in the mesoregions of *Norte maranhense*, *Agreste pernambuco*, *Mata pernambucana*, *Leste alagoano*, *Leste sergipano*, *Centro-Sul baiano* and *Sul baiano*. Moderate accuracies of between 20 and 40% were observed in 24 mesoregions in all states. *NRMSE* values of more than 40%, indicating low model accuracy, were observed in most of the mesoregions in the state of Ceará, with an average *NRMSE* of 43%, in *Sertão pernambucano*, *Borborema* and *Sertão sergipano*. In the *Central potiguar* mesoregion, the *NRMSE* was 52%, and the maximum value was observed in the *Sul maranhense* mesoregion, with *NRMSE* = 69%. Except for these two mesoregions with values exceeding 50%, the overall average *NRMSE* in all the other mesoregions was 29%, indicating a moderate prediction of the values simulated by the CCA model. It should be pointed out that a possible limiting factor in obtaining higher accuracies was the use of only one variable as a predictor of production—in this case, the cumulative six-month rainfall. Other factors are important for estimating production, such as other meteorological variables like temperature and solar radiation intensity, as well as other non-climatic factors that potentially influence production. The addition of meteorological variables other than rainfall in the construction of this model, for example, is a future objective of this research in the search for improvements in production estimates in the mesoregions of the NEB.

The map of correlations between observed and predicted production by the CCA model (Figure 7c) demonstrates its efficiency by raising all the *r* values obtained from the simple comparison between accumulated rainfall and production. There was an average increase of 27% in the *r* values. Of the 42 mesoregions among all the NEB states, in 39 the correlations between production simulated with CCA and observed, using the rainfall of the wettest semester as a predictor of production, were higher than the direct correlation between accumulated rainfall and production. The *RMSE*, *NRMSE* and *r* values are shown in detail in Table 2.

Table 2. For each mesoregion, correlation values (r) were obtained from the direct comparison of accumulated rainfall \times observed production, and the production simulated by the CCA model and observed. Values in bold highlight the highest r obtained.

| Mesoregion | r —Accumulated Rainfall \times Production | r —CCA Model \times Production | RMSE (kg/ha) | NRMSE (%) |
|--------------------------------------|--|------------------------------------|--------------|-----------|
| <i>Norte maranhense</i> | 0.45 | 0.74 | 68 | 13 |
| <i>Oeste maranhense</i> | 0.38 | 0.65 | 211 | 28 |
| <i>Central maranhense</i> | 0.47 | 0.66 | 247 | 37 |
| <i>Leste maranhense</i> | 0.44 | 0.66 | 143 | 30 |
| <i>Sul maranhense</i> | 0.37 | 0.56 | 1175 | 69 |
| <i>Norte piauiense</i> | 0.62 | 0.81 | 115 | 24 |
| <i>Centro Norte piauiense</i> | 0.66 | 0.82 | 129 | 27 |
| <i>Sudeste piauiense</i> | 0.71 | 0.83 | 188 | 38 |
| <i>Sudoeste piauiense</i> | 0.45 | 0.7 | 297 | 36 |
| <i>Noroeste cearense</i> | 0.33 | 0.78 | 99 | 22 |
| <i>Norte cearense</i> | 0.31 | 0.51 | 202 | 43 |
| <i>Metropolitana de Fortaleza</i> | 0.44 | 0.59 | 139 | 30 |
| <i>Sertões cearenses</i> | 0.5 | 0.7 | 218 | 43 |
| <i>Jaguaribe</i> | 0.37 | 0.53 | 274 | 44 |
| <i>Centro-Sul cearense</i> | 0.35 | 0.66 | 278 | 45 |
| <i>Sul cearense</i> | 0.5 | 0.73 | 343 | 41 |
| <i>Oeste potiguar</i> | 0.69 | 0.8 | 141 | 27 |
| <i>Central potiguar</i> | 0.64 | 0.52 | 153 | 52 |
| <i>Agreste potiguar</i> | 0.63 | 0.74 | 210 | 39 |
| <i>Leste potiguar</i> | 0.42 | 0.62 | 151 | 49 |
| <i>Sertão paraibano</i> | 0.43 | 0.76 | 231 | 48 |
| <i>Borborema</i> | 0.6 | 0.54 | 156 | 37 |
| <i>Agreste paraibano</i> | 0.63 | 0.65 | 208 | 30 |
| <i>Mata paraibana</i> | 0.5 | 0.56 | 105 | 20 |
| <i>Sertão pernambucano</i> | 0.76 | 0.53 | 832 | 39 |
| <i>São-Francisco pernambucano</i> | 0.39 | 0.65 | 134 | 20 |
| <i>Agreste pernambucano</i> | 0.75 | 0.81 | 109 | 30 |
| <i>Mata pernambucana</i> | 0.64 | 0.69 | 122 | 27 |
| <i>Metropolitana do Recife</i> | 0.35 | 0.48 | 123 | 27 |
| <i>Sertão alagoano</i> | 0.77 | 0.79 | 156 | 25 |
| <i>Agreste alagoano</i> | 0.62 | 0.63 | 86 | 20 |
| <i>Leste alagoano</i> | 0.2 | 0.42 | 54 | 13 |
| <i>Sertão sergipano</i> | 0.53 | 0.63 | 276 | 38 |
| <i>Agreste sergipano</i> | 0.43 | 0.67 | 591 | 48 |
| <i>Leste sergipano</i> | 0.34 | 0.71 | 266 | 27 |
| <i>Extremo oeste Baiano</i> | 0.17 | 0.68 | 103 | 13 |
| <i>Vale São Franciscano da Bahia</i> | 0.28 | 0.43 | 89 | 25 |
| <i>Centro-Sul baiano</i> | 0.16 | 0.67 | 124 | 22 |
| <i>Centro-Norte baiano</i> | 0.65 | 0.72 | 70 | 13 |
| <i>Nordeste baiano</i> | 0.62 | 0.67 | 52 | 6 |
| <i>Metropolitana de Salvador</i> | 0.36 | 0.68 | 150 | 24 |
| <i>Sul baiano</i> | 0.42 | 0.69 | 188 | 23 |

3.3. Results by State—Maranhão

The state of Maranhão has maize production in all mesoregions. In the period of analysis of this research, 1981–2010, the average produced in each mesoregion was 523 kg/ha in *Norte maranhense*, 746 kg/ha in *Oeste maranhense*, 670 kg/ha in *Central maranhense*, 474 kg/ha in *Leste maranhense* and 1710 kg/ha in *Sul maranhense*. The graphs in Figure 8 show the comparison between the production observed and simulated by the model in each mesoregion. There is good agreement between simulation and observation, especially in *Norte maranhense* (Figure 8a), with the model following the increase in observed production from 1995 onwards, although underestimating observations from 2000 onwards. This underestimation is also seen in *Oeste maranhense* (Figure 8b), which showed an upward

trend in production from 2000 onwards. In *Central maranhense*, the upward trend begins in 1998 and the model underestimates from 2003 onwards (Figure 8c), with a similar situation seen in *Leste maranhense* (Figure 8d). Finally, this characteristic of increased production is more pronounced in *Sul maranhense* (Figure 8e), as a result of the advance of the agricultural frontier called MATOPIBA, which has one of its most productive areas in the south of the state [37,38]. It is important to note that, in each mesoregion, especially in the *Sul maranhense*, before the increase in production, the model shows a positive bias, overestimating the observed production.

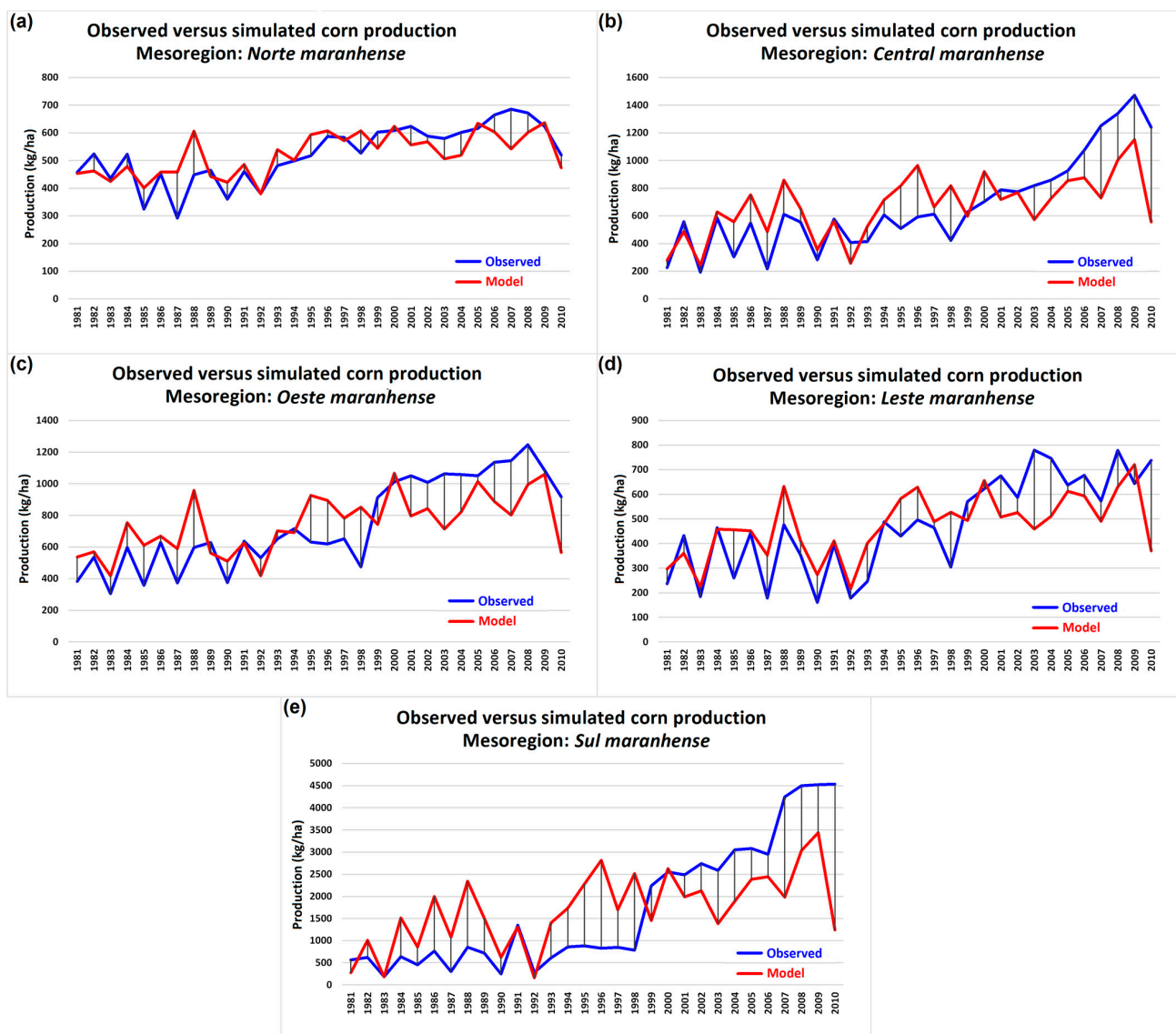


Figure 8. Production observed (blue line) and simulated with the CCA model (red line), for the period 1981–2010, for the mesoregions of Maranhão: (a) *Norte maranhense*, (b) *Oeste maranhense*, (c) *Central maranhense*, (d) *Leste maranhense* and (e) *Sul maranhense*.

3.4. Results by State—Piauí

The results of the model simulations for Piauí showed an excellent fit with the observations. The correlation values obtained were high: 0.81 for the *Norte piauiense* (Figure 9a), 0.82 for the *Centro-Norte piauiense* (Figure 9b), 0.83 for the *Sudoeste piauiense* (Figure 9c) and 0.70 for the *Sudeste piauiense* (Figure 9d). Average production in the period is similar between the *Norte piauiense*, *Centro-Norte piauiense*, and *Sudoeste piauiense* mesoregions, at around 480 kg/ha. In the *Sudeste piauiense*, it is around 825 kg/ha, as is the case for the south of

Maranhão, as a result of the MATOPIBA agricultural expansion [38], which has advanced in this mesoregion of Piauí; although soybeans are the mainstay of production [39,40], maize is also planted on a larger scale than in the other mesoregions of the state. Figure 8 shows that the model was able to simulate and capture most of the variation in production in all mesoregions. These results show that in Piauí, the response between the independent variable (accumulated rainfall) and the dependent variable (production) is more direct than in other mesoregions in other states. The rainfall regime in Piauí is associated with the southward shift of the ITCZ [41], with its interannual variations being decisive for the quality of the rainy season in the north of the NEB [42], being the main factor in the success or failure of crops. Furthermore, in the mesoregion of southwestern Piauí, rainfall events that occur from October to March [43] are equally important.

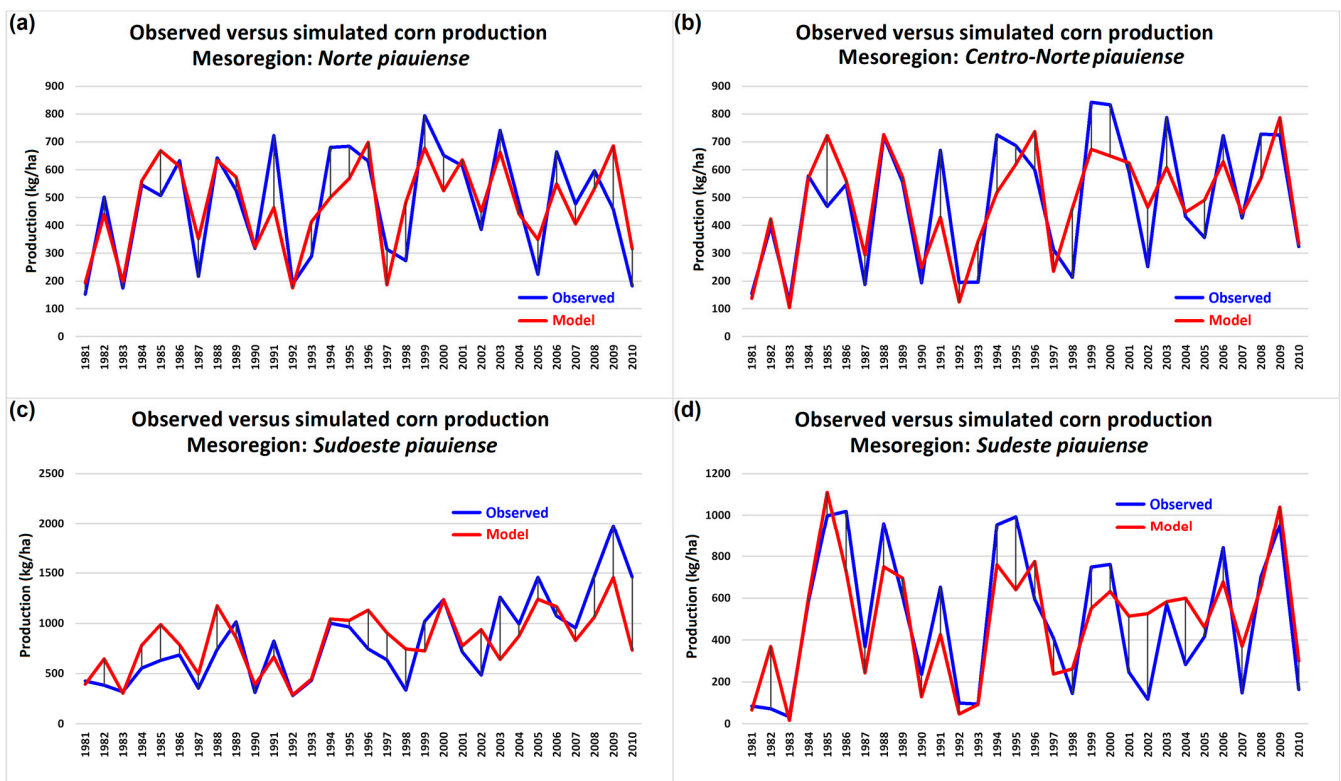


Figure 9. The same as Figure 8, but for the mesoregions of Piauí: (a) *Norte piauiense*, (b) *Centro-Norte piauiense*, (c) *Sudoeste piauiense* and (d) *Sudeste piauiense*.

3.5. Results by State—Ceará

Ceará has seven mesoregions (Figure 10), due to the dismemberment of the municipalities bordering the capital, which formed the *Metropolitana de Fortaleza* mesoregion (Figure 10b). Throughout the state, the wettest period is the JFMAMJ semester, influenced by systems such as upper tropospheric cyclonic vortices (UTCV), which peak between January and February [44], ITCZ between February and April [45], remnants of easterly wave disturbances (EWD) in May and June [46], in addition to the interaction between larger-scale phenomena, such as frontal systems that induce the formation of mesoscale convective complexes [47,48]. However, as in the entire northern sector of the NEB, there is great interannual variability and poor spatial-temporal distribution of rainfall in the growing season, reflecting in years with higher and lower production.

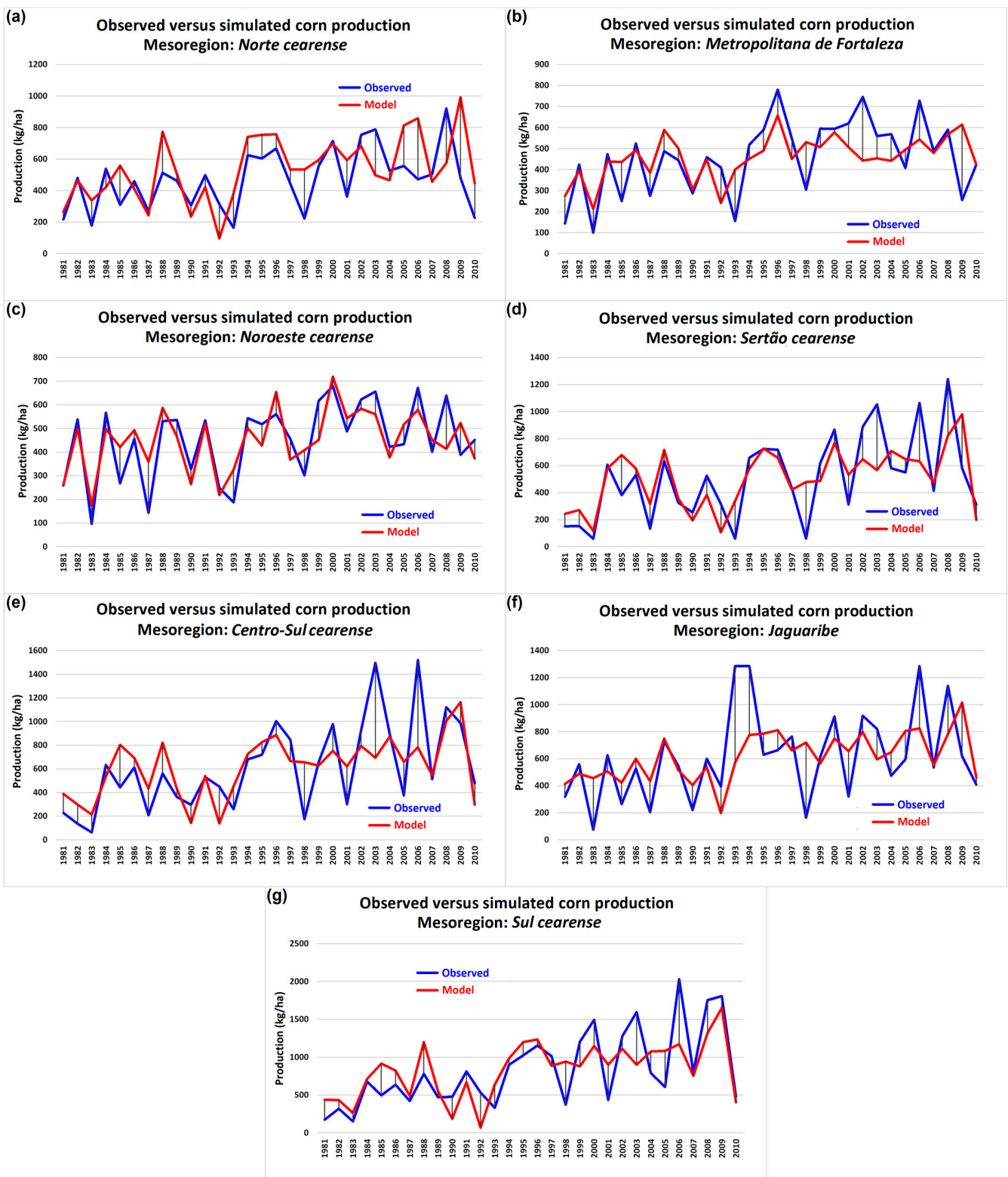


Figure 10. The same as in Figure 8, but for the mesoregions of Ceará: (a) *Norte cearense* (b) *Metropolitana de Fortaleza*, (c) *Noroeste cearense*, (d) *Sertão cearense*, (e) *Centro-Sul cearense*, (f) *Jaguaribe* and (g) *Sul cearense*.

This pattern of alternating more/less productive years (periods) was well captured by the model simulations in all mesoregions. Among these, the best performance based on correlations was seen in the *Sul cearense* (Figure 10g), followed by the *Sertão cearense*

(Figure 10d), *Centro-Sul cearense* (Figure 10e), the *Metropolitana de Fortaleza* (Figure 10b), *Jaguaribe* (Figure 10f) and the *Norte cearense* (Figure 10a).

3.6. Results by State—Rio Grande do Norte

In Rio Grande do Norte, the best performance of the simulations was seen in the *Oeste potiguar* and *Agriste potiguar* mesoregions, with correlations of 0.80 and 0.74, respectively (Figures 11a and 11c), following the trend of increased production from the mid-1990s onwards. The *Central potiguar* mesoregion (Figure 11b) showed the lowest correlation between simulations and observations, influenced by two positive peaks in the 1990 and 1993 observations not captured by the forecast model. The observed value estimated by the IBGE for 1993, in particular, is suspect due to all the other mesoregions showing low production values in that year, as can be seen most clearly in the *Leste potiguar* mesoregion (Figure 10d). The year 1993 was influenced by the continuation of a warm phase of ENOS (El Niño), classified as strong in the 1991–1992 biennium and weak in the 1992–1993 biennium, i.e., a sequence of three years under the influence of an extended El Niño, which on average reduces rainfall, especially in the states of the northern sector of the NEB [49].

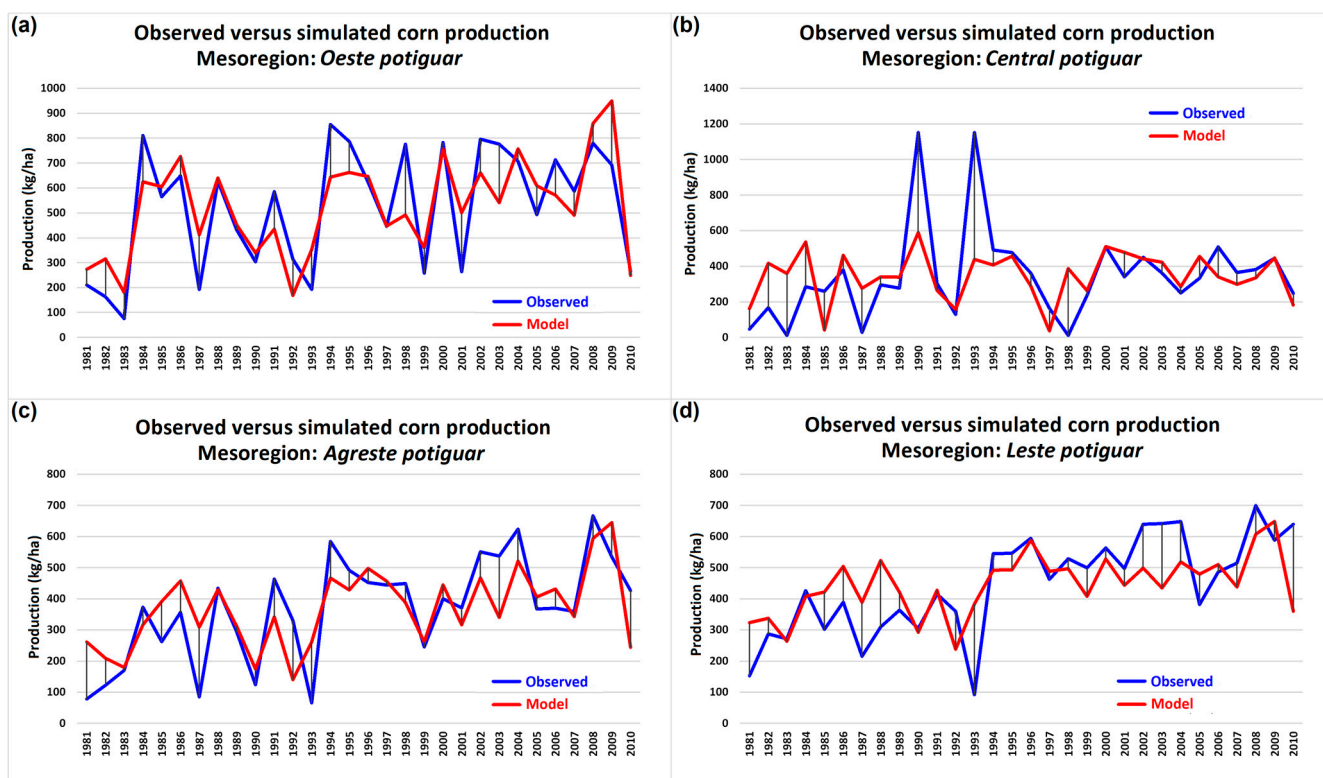


Figure 11. The same as in Figure 8, but for the mesoregions of Rio Grande do Norte: (a) *Oeste potiguar* (b) *Central potiguar*, (c) *Agriste potiguar*, and (d) *Leste potiguar*.

3.7. Results by State—Paraíba

As observed for Rio Grande do Norte, the western sector of Paraíba, in its *Sertão paraibano* mesoregion, showed the highest correlations between simulated and observed production ($r = 0.71$), followed by the *Agriste paraibano*, *Mata paraibana* and *Borborema* mesoregions, the latter of which is considered to be one of the areas with the lowest rainfall rates in Brazil [50]. The model’s ability to capture the observed behavior can be seen, although it has difficulty simulating some specific positive/negative peaks observed in the 1981–2010 period. Between 1994 and 1997, the model captured and simulated the above-average observations well, most clearly in the *Sertão* (Figure 12a), *Borborema* (Figure 12b) and *Agriste* (Figure 12c) mesoregions. The *Mata paraibana* mesoregion (Figure 12d) showed a peak in observed production in 2003 which was not captured by the model. Unlike the peak

observed in 1993 in the central mesoregion of Rio Grande do Norte, this is not a suspicious value, as it was also a year of high production values observed in the *Agreste* mesoregion.

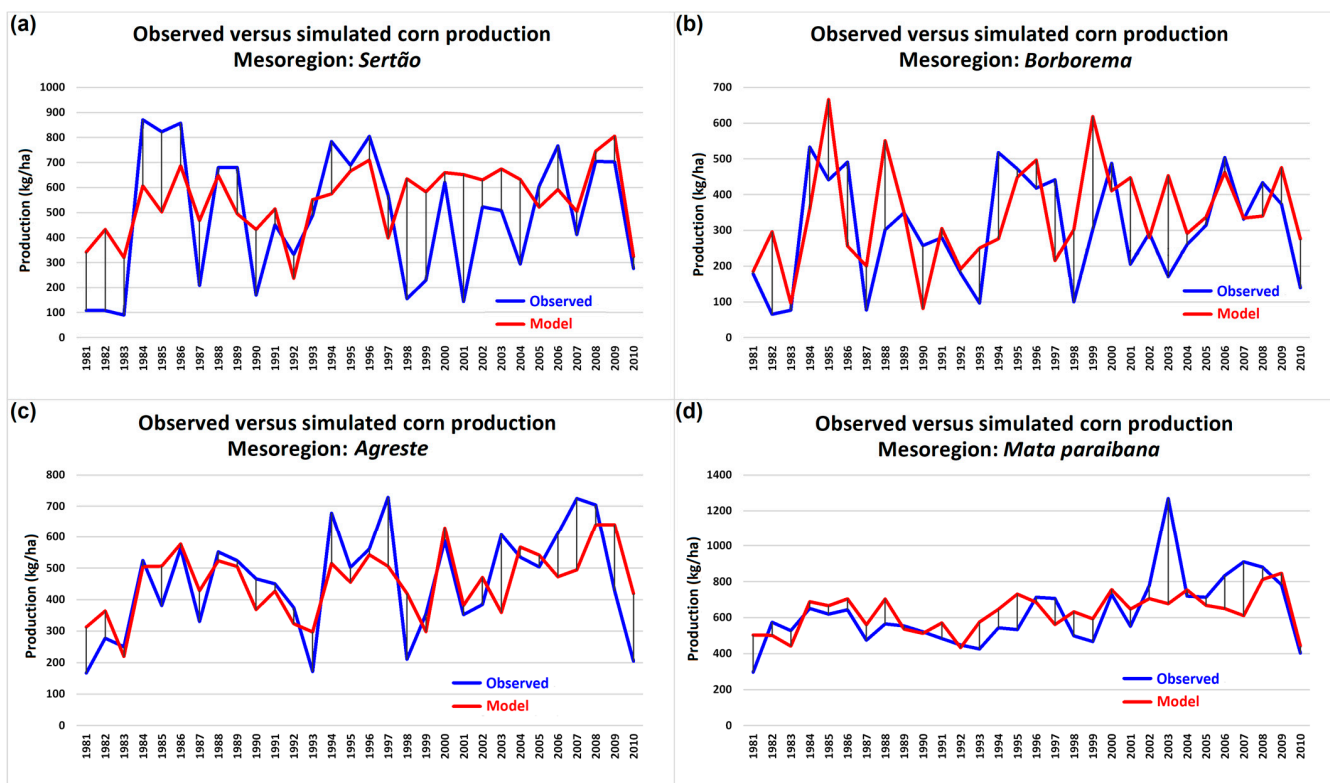


Figure 12. The same as in Figure 8, but for the mesoregions of Paraíba: (a) *Sertão*, (b) *Borborema*, (c) *Agreste* and (d) *Mata paraibana*.

3.8. Results by State—Pernambuco

Maize production is very homogeneous in four of Pernambuco’s five mesoregions, with average values of 480 kg/ka in Pernambuco’s *Sertão* (Figure 13a), 428 kg/ha in the *São-Francisco Pernambucano* (Figure 13b), 437 kg/ha in the *Agreste* (Figure 13c) and 424 kg/ha in the *Zona da Mata* (Figure 13d), with only the *Metropolitana de Recife* mesoregion differing from this homogeneity with an average production of 725 kg/ha (Figure 13d).

The model simulated the observations well, without preferential bias, with the highest correlation with observations obtained for the *Agreste* ($r = 0.81$), and the lowest in the *Metropolitana de Recife* mesoregion ($r = 0.48$). The low maize yields in most of Pernambuco’s mesoregions reflect the practice of rainfed agriculture and the fact that this is one of the Northeastern states with the highest rate of return from moderate to severe droughts [25,51].

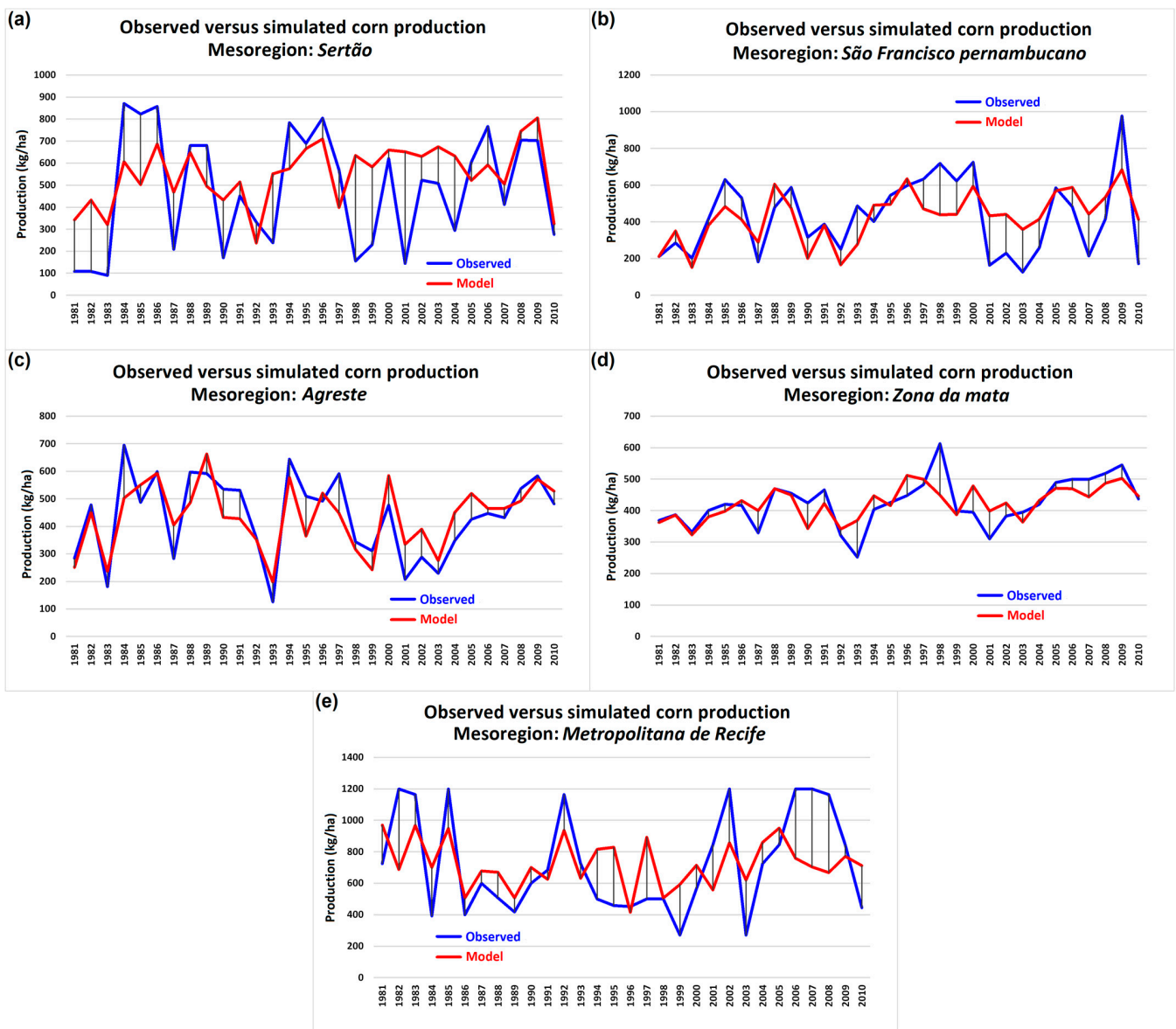


Figure 13. The same as in Figure 8, but for the mesoregions of Pernambuco: (a) *Sertão*, (b) *São Francisco pernambucano*, (c) *Agreste*, (d) *Zona da Mata* and (e) *Metropolitana de Recife*.

3.9. Results by State—Alagoas and Sergipe

Alagoas and Sergipe are two states in the east of the Northeast with similarities between them. Both have three mesoregions, *Sertão*, *Agreste* and *Leste*, and they have the same climate regime, with the wettest period, or growing season, from April to September, whose greatest influence on the precipitation regime is due to the transport of moisture from the Atlantic Ocean by the east/southeast trade winds, which are often associated with EWDs [46]. Kouadio et al. [52] evaluated extreme rainfall events in the eastern NEB and investigated their climatic causes, concluding that phenomena of different natures on different time scales are responsible for the rainfall dynamics in this region, such as ENOS, the Atlantic dipole and the Pacific decadal oscillation.

However, grain production, in this case maize, shows differences between the mesoregions of these states in the period analyzed. Alagoas has an average production of 359 kg/ha in the *Sertão* mesoregion (Figure 14a), 567 kg/ha in the *Agreste* mesoregion (Figure 14b), and 533 kg/ha in the *Leste* mesoregion (Figure 14c), which are lower than the values observed for Sergipe, with an average production of 1239 kg/ha in the *Sertão*

(Figure 15a), 997 kg/ha in the *Agreste* (Figure 15b), and 773 kg/ha in the *Leste* (Figure 15c). The differences in the *Leste* and *Agreste* sectors can be explained by the greater predominance of sugar cane cultivation in these mesoregions of Alagoas than in Sergipe [53]. However, the large difference observed in production in the *Sertão* mesoregion of each state needs to be better investigated. In [54], da Silva et al. cite the incentives of agricultural credit and soil type as determining factors for the expansion of maize cultivation in Sergipe, and policies relating to the effect of Agricultural Climate Risk Zoning, a Brazilian agricultural policy that exerted a superior effect on maize productivity in the *Sertão* compared to neighboring municipalities in other mesoregions [55].

It is worth noting that the entire *Agreste* and *Leste* of these states, and the northeastern mesoregion of Bahia, have been experiencing strong growth in terms of agricultural expansion, in a new agricultural frontier called SEALBA [56], with high potential for mechanized agriculture. Such effects of grain production in SEALBA, such as maize, occurred after 2010, so this effect has not yet been detected in the analysis period of this research, 1981–2010.

The models best simulated the variability of maize production in the mesoregions of *Sertão* of Alagoas ($r = 0.79$) and *Leste* of Sergipe ($r = 0.71$). In the other mesoregions, it was efficient at following trends and some peaks in observed production.

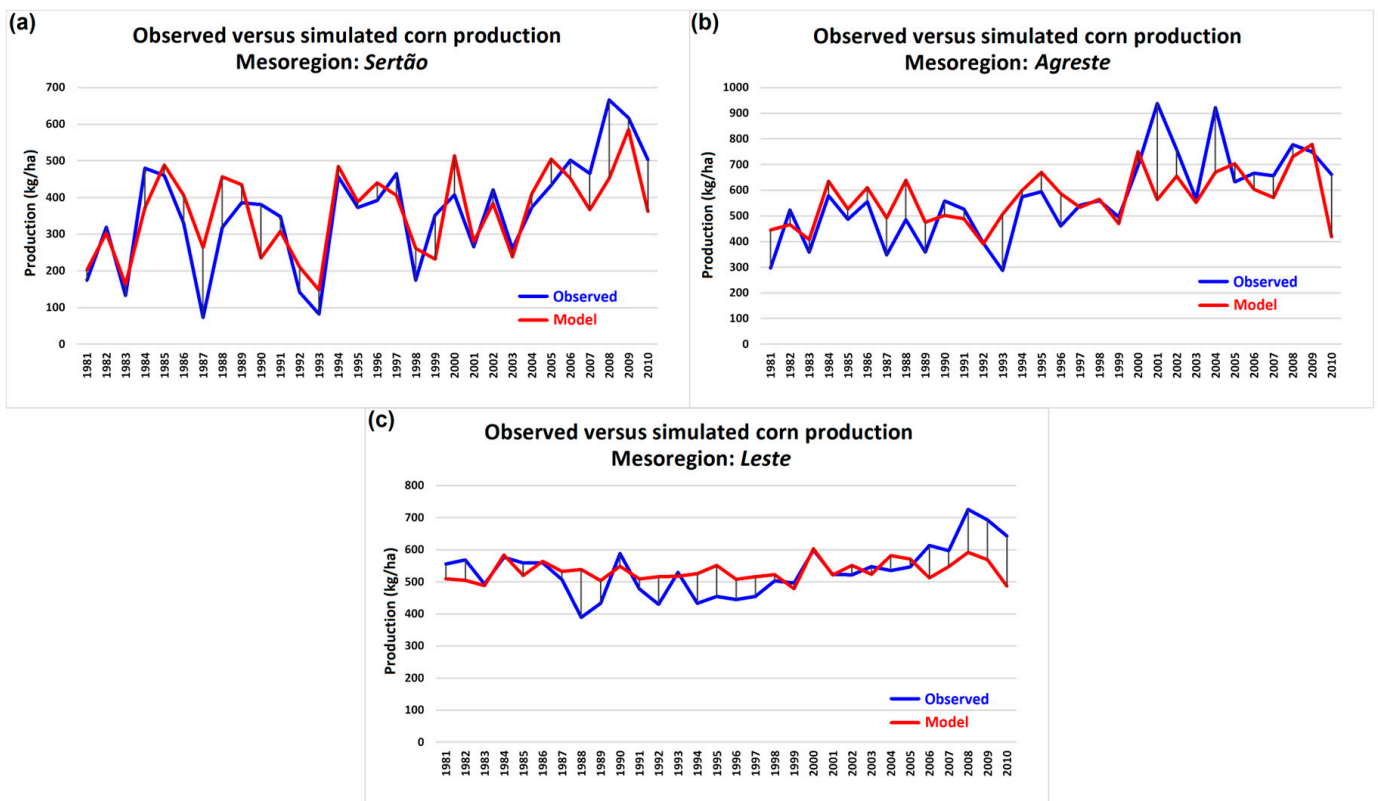


Figure 14. The same as in Figure 8, but for the mesoregions of Alagoas: (a) *Sertão*, (b) *Agreste*, and (c) *Leste*.

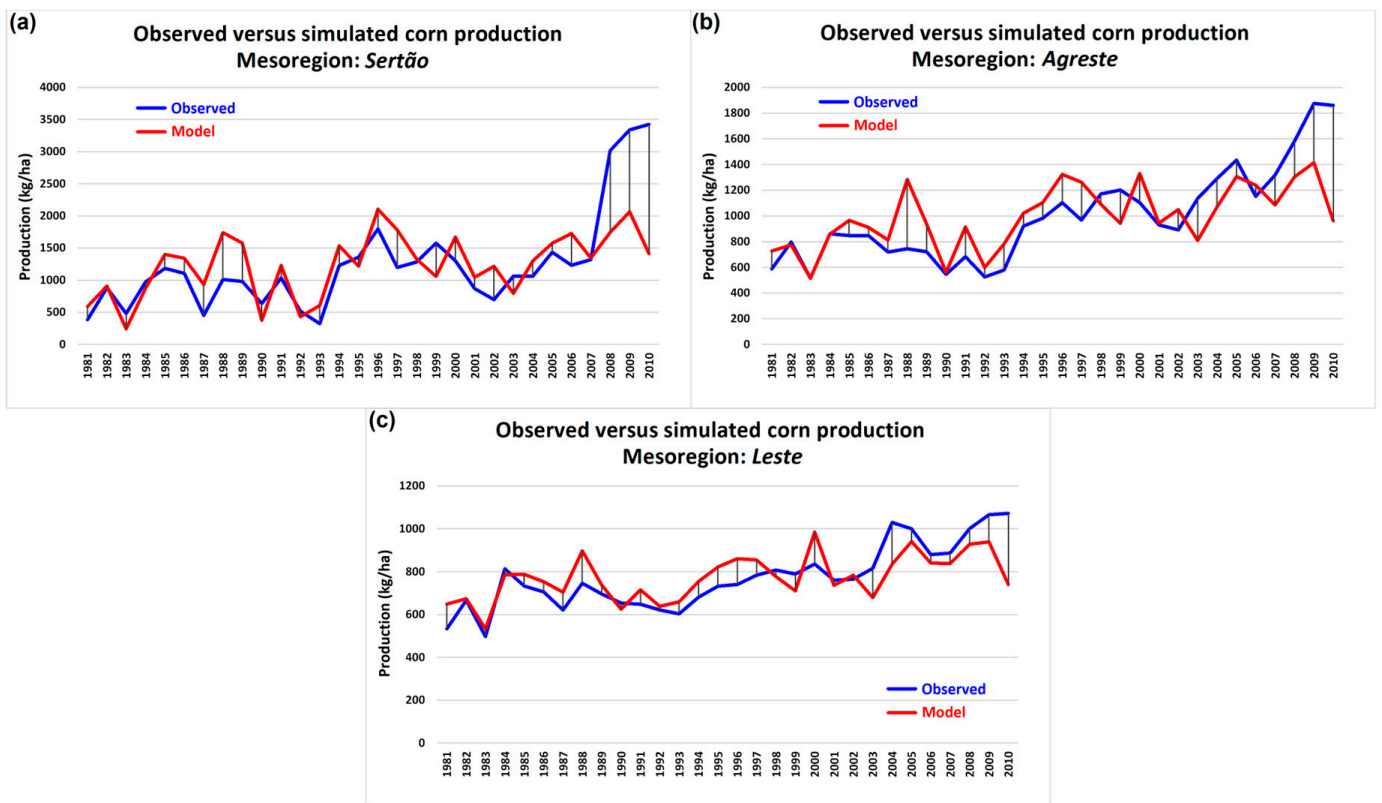


Figure 15. The same as in Figure 8, but for the mesoregions of Sergipe: (a) *Sertão*, (b) *Agreste*, and (c) *Leste*.

3.10. Results by State—Bahia

The largest state in the NEB, Bahia has seven mesoregions: *Extremo oeste baiano*, *Vale são-franciscano baiano*, *Nordeste baiano*, *Centro-norte baiano*, *Metropolitana de Salvador*, *Centro-Sul baiano* and *Sul baiano*. Average production from 1981 to 2010 ranged from 521 kg/ha in the *Centro-Norte baiano* to 2158 kg/ha in the *Extremo oeste baiano*, around 650 kg/ha in the *Vale São-Franciscano baiano*, the *Centro-Sul baiano* and the *Nordeste baiano*, and around 820 kg/ha in the *Metropolitana de Salvador* and the *Sul baiano*. Due to its size and different forms of cultivation, Bahia is a classic example of a state that has three distinct productivity classes: high productivity in the far west, related to the area of the state that is part of MATOPIBA [57], moderate productivity in the *Sul baiano* and the *Metropolitana de Salvador*, and low productivity in the other mesoregions.

The biggest challenge in developing any model is having it capture random peaks and trends in a time series. In this more specific case, the challenge would be for the model to capture the abrupt change in the level of productivity observed in *Extremo oeste baiano* from the 1990s onwards with the advance of the agricultural frontier in this sector of the state [58].

Figure 16a shows the simulation versus observation in the *Extremo oeste baiano*, and it is clear that the model has captured the new average production level, which jumped from an average of around 1000 kg/ha between 1981 and 1990 to an average of around 2700 kg/ha between 1991 and 2010, with a tendency to increase again towards the end of the series, with a correlation of 0.68 between simulated and observed values.

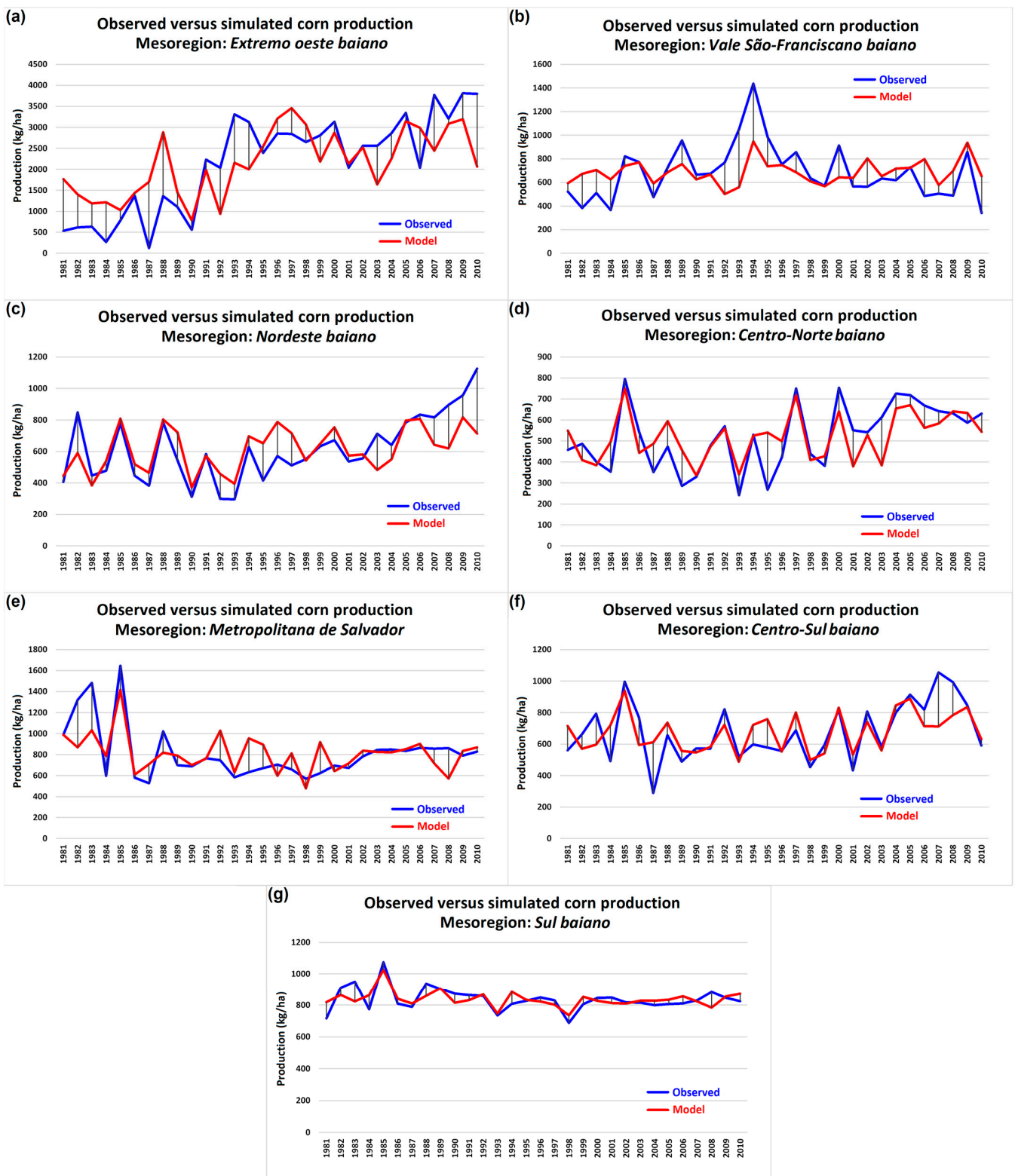


Figure 16. The same as in Figure 8, but for the mesoregions of Bahia: (a) *Extremo oeste baiano*, (b) *Vale São-Franciscano baiano*, (c) *Nordeste baiano*, (d) *Centro-Norte baiano*, (e) *Metropolitana de Salvador*, (f) *Centro-Sul baiano* and (g) *Sul baiano*.

In the other mesoregions, as observed in the analyses for the other states, it can be seen that the model is capable and simulates the observed behavior well. The correlations between simulations and observations were 0.43 in the *Vale São-Franciscano baiano*, the

lowest among the mesoregions (Figure 16b), 0.67 in the Nordeste baiano (Figure 16c), 0.72 in the *Centro-Norte baiano* (Figure 16d), 0.69 in the Metropolitana de Salvador (Figure 16e), 0.67 in the *Centro-Sul baiano* (Figure 16f), and 0.69 in the *Sul baiano* (Figure 16g).

3.11. Ocean-Atmosphere Interaction versus Production

Analysis of the performance of the CCA-based model showed that, in all the mesoregions of the NEB, the observed annual production of maize can be well simulated by this type of statistical modeling. It was also observed that there was a great deal of inter-annual variability in production, which was well captured by the model. However, the climate of the NEB is complex, and the distribution of rainfall is the response of various oceanic and atmospheric phenomena connected to each other. Classic studies have already demonstrated the relationship between the El Niño-Southern Oscillation (ENOS) and the intraseasonal and interannual variability of the ITCZ [59,60]. The dipole of sea surface temperature anomalies in the North and South Atlantic (DIP) also has a strong influence on the rainfall dynamics of the NEB [61,62]. As these phenomena in their different phases occur simultaneously, there are up to nine different combinations when relating the phases of ENOS and DIP: negative DIP + negative Pacific (La Niña), negative DIP + neutral Pacific, negative DIP + positive Pacific (El Niño), neutral DIP + negative Pacific, neutral DIP + neutral Pacific, neutral DIP + positive Pacific, positive DIP + negative Pacific, positive DIP + neutral Pacific and positive DIP + positive Pacific.

Each year between 1981 and 2010 was classified based on these combinations, as shown in Table 3. Then, the percentage deviations of the average production for each pair of combinations were obtained concerning the average production observed for each mesoregion in the 1981–2010 period. The classification of the Pacific phases was based on the Oceanic Niño Index (ONI, https://origin.cpc.ncep.noaa.gov/products/analysis_monitoring/ensostuff/ONI_v5.php (accessed on 5 August 2023)), described in [63], and of the DIP phases on the difference between SST anomalies in an area of the North Atlantic from 5.5° N to 23.5° N and from 15° W to 57.5° W, with SST anomalies in the South Atlantic from 0° to 20° S and from 10° E to 20° W (<https://psl.noaa.gov/data/correlation/tna.data>; <https://psl.noaa.gov/data/correlation/tsa.data> (accessed on 5 August 2023)) [64,65].

Table 3. Composite years are classified according to the definitions of the climatic events observed in the Pacific and Atlantic oceans. DIP: Atlantic dipole; Pac: Pacific; Neg: negative; Neu: neutral; Pos: positive.

| Climate Combinations | Years |
|----------------------|------------------------------------|
| DipNeg/PacNeg | 1984, 1985, 1986, 1989, 2000, 2008 |
| DipNeg/PacNeu | 1991, 1994 |
| DipNeg/PacPos | 1988, 1995, 2003, 2009, 2010 |
| DipNeu/PacNeg | 1996, 1999 |
| DipNeu/PacNeu | 1982, 1990, 1993, 2004 |
| DipNeu/PacPos | 1987, 1998, 2002, 2006, 2007 |
| DipPos/PacNeg | 1997 |
| DipPos/PacNeu | 1980, 1981, 2001, 2005 |
| DipPos/PacPos | 1983, 1992 |

Figure 17 shows the average percentage yield deviations for the DipNeg/PacNeg (a), DipNeg/PacNeu (b) and DipNeg/PacPos (c) combinations. The mesoregions in the semi-arid interior between the states of Piauí, Ceará, Rio Grande do Norte, Paraíba and Pernambuco mostly showed yield gains, with the exception of the *Norte*, *Oeste* and *Sul maranhense*, and *Extremo oeste baiano* for the negative dipole and negative Pacific combination (Figure 17a), all the mesoregions of Maranhão, central-eastern Bahia, Sergipe and Alagoas (*Agreste* and *Leste* mesoregions) for the negative dipole and neutral Pacific combination (Figure 17b). The combination of years with a negative dipole and a positive Pacific was the one in which most of the mesoregions showed an average increase in production, especially the whole of the north of the NEB, Alagoas and Sergipe in the east of the NEB,

and the mesoregions of western Bahia, the *Vale São-Franciscano baiano*, the *Nordeste baiano*, *Metropolitana de Salvador* and *Sul baiano* (Figure 17c), reaching more than 60% with the average in the *Sertão* mesoregion of Sergipe.

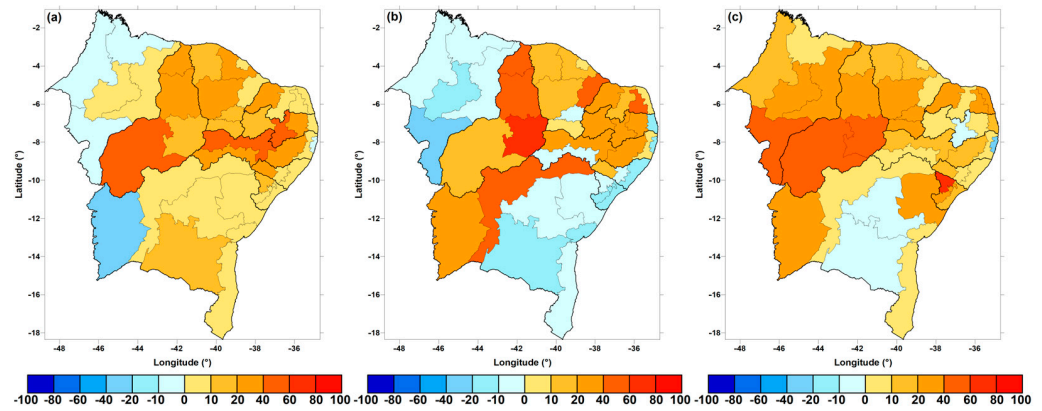


Figure 17. Average deviation of production from the 1981–2010 average for years classified under the influence of the negative Atlantic dipole and (a) negative Pacific, (b) neutral Pacific and (c) positive Pacific.

Under neutral DIP conditions, most of the mesoregions in the north of the NEB show positive deviations in production in relation to the average, while the opposite occurs in most of the mesoregions in the east of the NEB (Figure 18a). For the combination of neutral DIP and neutral Pacific, except for a few mesoregions which showed a low positive deviation in production, most mesoregions showed negative deviations, i.e., production below the average, of up to -60% in the *Sudeste piauiense* (Figure 18b). The combination of neutral DIP and positive Pacific does not show homogeneity, with mesoregions alternating positive and negative deviations, with the negative deviations more concentrated in the mesoregions of Piauí and Pernambuco, and the positive deviations in *Centro-Oeste maranhense*, *Centro-Sul cearense*, and the far east of the NEB (Figure 18c).

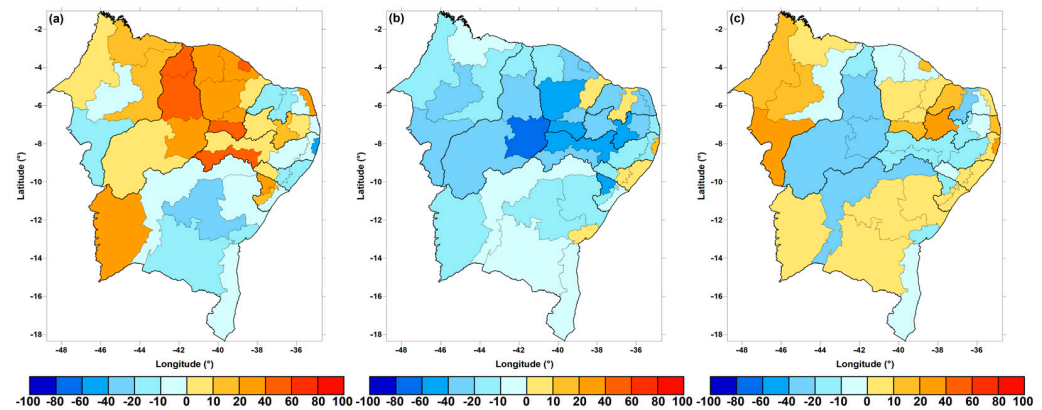


Figure 18. Average deviation of production from the 1981–2010 average for years classified under the influence of the neutral Atlantic dipole and (a) negative Pacific, (b) neutral Pacific and (c) positive Pacific.

Finally, there is the analysis of the combinations for positive DIP and Pacific phases. For positive DIP and negative Pacific, the western portion of the NEB, which involves most of the mesoregions of Maranhão, Piauí, and some of Ceará, Rio Grande do Norte and Paraíba, showed on average a reduction in the percentage of production, a fact also observed in the mesoregions of the eastern NEB from Pernambuco to Bahia (Figure 19a). The combination of positive DIP and neutral Pacific (Figure 19b) already showed most of the central-eastern NEB with negative deviations in production, with the notable exception of mesoregions in Maranhão and the *Sudoeste piauiense*. The combination of positive DIP and positive Pacific represented the most damaging situation for maize production, exceeding

–80% in *Sul maranhense* and *Sudeste piauiense*, with the exception of the *Centro-Sul baiano*, *Metropolitana de Salvador* and *Sul baiano* mesoregions (Figure 19c).

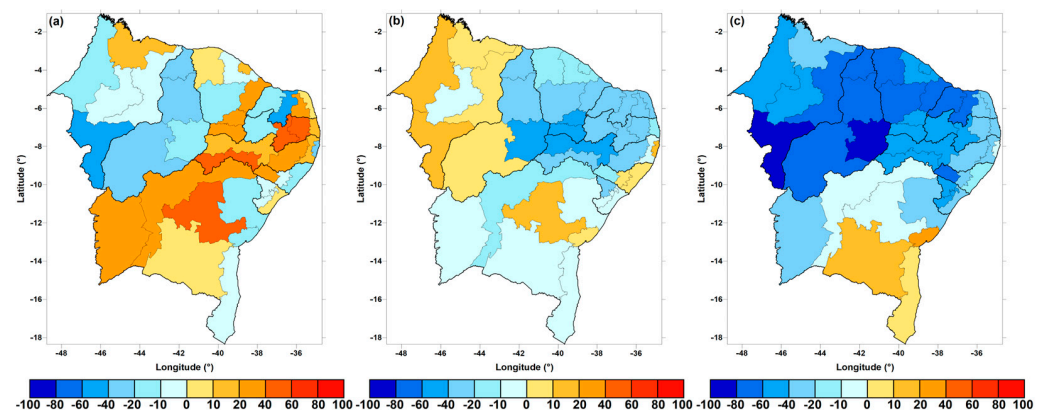


Figure 19. Average deviation of production from the 1981–2010 average for years classified under the influence of a positive Atlantic dipole and (a) negative Pacific, (b) neutral Pacific and (c) positive Pacific.

This fact has already been investigated, and the results for this last combination are in line with the results obtained by [66], when they investigated the influence of the different phases of the Pacific and Atlantic on maize and bean production in Ceará between 1952 and 2000.

4. Conclusions

The CCA-based model, relating predictor (accumulated rainfall in the wettest semester, or “growing season”) and predictand (maize production by NEB mesoregion), showed moderate to high correlations in most mesoregions, corroborating its effectiveness in capturing the behavior of the time series of observations. It was observed that there were already statistically significant correlations simply relating accumulated rainfall to production, but the CCA model presented simulations with behavior more consistent with that of the observed values, increasing the correlation when using accumulated rainfall as a predictor of observed production. The *RMSE* used to assess the magnitude of the model’s errors showed an average error across all mesoregions of around 200 kg/ha, with some more extreme values in specific mesoregions, such as *Sul maranhense* and *Extremo oeste baiano*. The *NRMSE*, used to assess the accuracy of the values simulated by the model, showed high accuracy in the simulations in six mesoregions (*NRMSE* < 20%) and low accuracy in two mesoregions (*NRMSE* > 50%), with moderate accuracy in general in the remaining mesoregions, with an average value of *NRMSE* = 29%.

There is a well-defined statistical relationship between the climate variability of the tropical oceans (Pacific and Atlantic) and maize production, which should be similar to that of other crops. For rainfed agriculture, as is the case with most family farming in the NEB, in general for years with the combination of a negative Atlantic dipole and a negative Pacific (La Niña), there were positive deviations in production concerning the average, which was repeated even in the combination of a negative dipole and a positive Pacific (El Niño). This shows that the TSM conditions in the Atlantic tend to have a greater impact on the NEB’s climate than those in the Pacific, possibly inhibiting the negative effects (reduced rainfall) associated with weak and/or moderate El Niño events, since studies have already shown that in exceptional cases of very strong El Niños, their influence on reducing rainfall in the NEB is greater than the influence of a negative dipole condition. For neutral Atlantic dipole conditions, the most significant results came from the combination with a negative Pacific, which resulted in positive deviations in production in the north of the NEB, and a surprising result came from the combination of a neutral dipole and neutral Pacific, with a reduction (negative percentage deviations) in production in most of the northeastern mesoregions.

Finally, analyzing the three combinations of the Pacific and the positive Atlantic dipole, the result of negative deviations in production for the positive dipole and positive Pacific (El Niño) was confirmed, with the greatest effect for the north of the NEB, with some mesoregions showing relative losses of over 90% concerning the observed average production for the period.

Author Contributions: Conceptualization, F.D.d.S.S., I.C.P. and R.L.C.; methodology, F.D.d.S.S., I.C.P. and R.L.C.; software, F.D.d.S.S., I.C.P., R.L.C., H.B.G. (Helber Barros Gomes) and D.L.H.; validation, F.D.d.S.S.; formal analysis, F.D.d.S.S., I.C.P., R.L.C., H.B.G. (Helber Barros Gomes), H.B.G. (Heliofábio Barros Gomes), J.B.C.J., R.M.d.A. and D.L.H.; data curation, F.D.d.S.S.; writing—original draft preparation, F.D.d.S.S., I.C.P. and R.L.C.; writing—review and editing, F.D.d.S.S., I.C.P., R.L.C., H.B.G. (Helber Barros Gomes), H.B.G. (Heliofábio Barros Gomes), J.B.C.J., R.M.d.A. and D.L.H.; visualization, H.B.G. (Helber Barros Gomes), H.B.G. (Heliofábio Barros Gomes), J.B.C.J., R.M.d.A. and D.L.H.; funding acquisition, D.L.H. All authors have read and agreed to the published version of the manuscript.

Funding: This research received no external funding.

Data Availability Statement: The data used in the manuscript are available by writing to the corresponding authors.

Acknowledgments: We would like to thank all the institutions that made the data used in this research available free of charge. The first author would like to thank the financial support provided by FAPEAL (*Fundação de Amparo à Pesquisa de Alagoas*), through Notice n° E:002/2022, Process: E:60030.0000002510/2022. The second author would like to thank CAPES, which provided financial support in the form of a scholarship.

Conflicts of Interest: The authors declare no conflicts of interest.

References

1. CONAB—Companhia Nacional de Abastecimento. Acompanhamento da Safra Brasileira de Grãos, safra 1019/20 (Quinto levantamento). Brasília, DF, v. 7 (5), 1–112; 2020. Available online: https://www.conab.gov.br/info-agro/safras/graos/boletim-da-safra-de-graos/item/download/45055_d5c43cb0752e5b39bc31987286081f88 (accessed on 5 August 2023).
2. CONAB—Companhia Nacional de Abastecimento. Acompanhamento da Safra Brasileira de Grãos, safra 2023/24 (Quarto levantamento). Brasília, DF, v. 11 (4), 1–111; 2024. Available online: https://www.conab.gov.br/info-agro/safras/graos/boletim-da-safra-de-graos/item/download/51274_e40f1bba791d27a4c67a29c5f29781ff (accessed on 1 February 2024).
3. Bothast, R.J.; Schlicher, M.A. Biotechnological processes for conversion of corn into ethanol. *Appl. Microbiol. Biotechnol.* **2005**, *67*, 19–25. [CrossRef]
4. ABIMILHO. Associação Brasileira das Indústrias de Milho. Milho. 2020. Available online: <http://www.abimilho.com.br/milho/cereal> (accessed on 25 November 2023).
5. Divide, A.C.P.; Ribeiro, R.L.D.; Valle, T.L.; Almeida, D.L.; Castro, C.M.; Feltran, J.C. Produtividade de raízes de mandioca consorciada com milho e caupi em sistema orgânico. *Bragantia* **2009**, *68*, 145–153. [CrossRef]
6. Souza, A.E.; Reis, J.G.M.; Raymundo, J.C.; Pinto, R.S. Estudo da produção do milho no Brasil. *S. Am. Dev. Soc. J.* **2018**, *4*, 182–194. [CrossRef]
7. Garnett, E.R.; Khandekar, M.L. The impact of large-scale atmospheric circulations and anomalies on Indian monsoon droughts and floods and on world grain yields—A statistical analysis. *Agric. For. Meteorol.* **1992**, *61*, 113–128. [CrossRef]
8. Silva, B.K.d.N.; Costa, R.L.; Silva, F.D.d.S.; Vanderlei, M.H.G.d.S.; da Silva, H.J.F.; Júnior, J.B.C.; Costa Júnior, D.S.d.; Pedra, G.U.; Pérez-Marin, A.M.; Silva, C.M.S.e. Proposal of an Agricultural Vulnerability Stochastic Model for the Rural Population of the Northeastern Region of Brazil. *Climate* **2023**, *11*, 211. [CrossRef]
9. Cavalcante, E.S.; Lacerda, C.F.; Costa, R.N.T.; Gheyi, H.R.; Pinho, L.L.; Bezerra, F.M.S.; Oliveira, A.C.; Canjá, J.F. Supplemental irrigation using brackish water on maize in tropical semi-arid regions of Brazil: Yield and economic analysis. *Sci. Agric.* **2021**, *78*, e20200151. [CrossRef]
10. Cruz, J.C.; Pereira Filho, I.A.; Alvarenga, R.C.; Gontijo Neto, M.M.; Viana, J.H.M.; de Oliveira, M.F.; Matrangolo, W.J.R.; de Albuquerque Filho, M.R. EMBRAPA Milho e Sorgo: Cultivo do Milho, Sistemas de Produção, v. 2 (6). 2010. Available online: <https://ainfo.cnptia.embrapa.br/digital/bitstream/item/27037/1/Plantio.pdf> (accessed on 5 January 2024).
11. Coelho, D.T.; Dale, R.F. An energy-crop growth variable and temperature function for predicting corn growth and development: Planting to silking. *Agron. J.* **1980**, *72*, 503–510. [CrossRef]
12. Bonhomme, R. Bases and limits to using “degree-day” units. *Eur. J. Agron.* **2000**, *13*, 1–10. [CrossRef]

13. Guissem, J.M.; Sans, L.M.A.; Nakagawa, J.; Cruz, J.C.; Pereira Filho, I.A.; Mateus, G.P. Crescimento e desenvolvimento da cultura do milho (*Zea mays* L.) em semeadura tardia e sua relação com graus-dia e radiação solar global. *Rev. Bras. Agrometeorol.* **2001**, *9*, 215–260.
14. Streck, N.A.; Lago, I.; Gabriel, L.F.; Samboranza, F.K. Simulating maize phenology as a function of air temperature with a linear and a nonlinear model. *Pesqui. Agropecuária Bras.* **2008**, *43*, 449–455. [[CrossRef](#)]
15. Lacerda, F.F.; Nobre, P.; Sobral, M.C.; Lopes, G.M.B.; Chou, S.C.; Assad, E.D.; Brito, E. Long-term temperature and rainfall trends over northeast Brazil and Cape Verde. *Earth Sci. Clim. Chang.* **2015**, *6*, 296.
16. Oliveira, P.T.; Santos e Silva, C.M.; Lima, K.C. Climatology and trend analysis of extreme precipitation in subregions of Northeast Brazil. *Theor. Appl. Climatol.* **2016**, *130*, 77–90. [[CrossRef](#)]
17. Martins, M.A.; Tomasella, J.; Rodriguez, D.A.; Alvalá, R.C.; Giarolla, A.; Garofolo, L.L.; Júnior, J.L.S.; Paolicchi, L.T.; Pinto, G.L. Improving drought management in the Brazilian semiarid through crop forecasting. *Agric. Syst.* **2018**, *160*, 21–30. [[CrossRef](#)]
18. Martins, M.A.; Tomasella, J.; Dias, C.G. Maize yield under a changing climate in the Brazilian Northeast: Impacts and adaptation. *Agric. Water Manag.* **2019**, *216*, 339–350. [[CrossRef](#)]
19. Marengo, J.A.; Torres, R.R.; Alves, L.M. Drought in Northeast Brazil—past, present, and future. *Theor. Appl. Climatol.* **2016**, *129*, 1189–1200. [[CrossRef](#)]
20. Cunha, A.P.M.A.; Alvalá, R.C.S.; Nobre, C.A.; Carvalho, M.A. Monitoring vegetative drought dynamics in the Brazilian semiarid Region. *Agric. For. Meteorol.* **2015**, *214*, 494–505. [[CrossRef](#)]
21. Cunha, A.P.M.A.; Tomasella, J.; Ribeiro-Neto, G.G.; Brown, M.; Garcia, S.R.; Brito, S.B.; Carvalho, M.A. Changes in the spatial-temporal patterns of droughts in the Brazilian Northeast. *Atmos. Sci. Lett.* **2018**, *19*, e855. [[CrossRef](#)]
22. Cunha, A.P.M.A.; Zeri, M.; Leal, K.D.; Costa, L.; Cuartas, L.A.; Marengo, J.A.; Tomasella, J.; Vieira, R.M.; Barbosa, A.A.; Cunningham, C.; et al. Extreme Drought Events over Brazil from 2011 to 2019. *Atmosphere* **2019**, *10*, 642. [[CrossRef](#)]
23. Alvala, R.C.S.; Cunha, A.P.M.A.; Brito, S.S.B.; Seluchi, M.E.; Marengo, J.A.; Moraes, O.L.L.; Carvalho, M.A. Drought monitoring in the Brazilian Semiarid region. *An. Acad. Bras. Ciências* **2017**, *91*, e20170209. [[CrossRef](#)]
24. Medeiros, F.J.; Oliveira, C.P.; Avila-Diaz, A. Evaluation of extreme precipitation climate indices and their projected changes for Brazil: From CMIP3 to CMIP6. *Weather Clim. Extrem.* **2022**, *38*, 100511. [[CrossRef](#)]
25. Pontes Filho, J.D.; Souza Filho, F.d.A.; Martins, E.S.P.R.; Studart, T.M.d.C. Copula-Based Multivariate Frequency Analysis of the 2012–2018 Drought in Northeast Brazil. *Water* **2020**, *12*, 834. [[CrossRef](#)]
26. Marengo, J.A.; Galdos, M.V.; Challinor, A.; Cunha, A.P.; Marin, F.R.; Vianna, M.S.; Alvala, R.C.S.; Alves, L.M.; Moraes, O.L.; Bender, F. Drought in Northeast Brazil: A review of agricultural and policy adaptation options for food security. *Clim. Resil. Sustain.* **2021**, *1*, e17. [[CrossRef](#)]
27. Costa, R.L.; Barros Gomes, H.; Cavalcante Pinto, D.D.; da Rocha Júnior, R.L.; dos Santos Silva, F.D.; Barros Gomes, H.; Lemos da Silva, M.C.; Luís Herdies, D. Gap Filling and Quality Control Applied to Meteorological Variables Measured in the Northeast Region of Brazil. *Atmosphere* **2021**, *12*, 1278. [[CrossRef](#)]
28. Mason, S.J.; Tippet, M.K. (Eds.) *Climate Predictability Tool Version 15.5.10*; Columbia University Academic Commons: New York, NY, USA, 2017.
29. Esquivel, A.; Llanos-Herrera, L.; Agudelo, D.; Prager, S.D.; Fernandes, K.; Rojas, A.; Valencia, J.J.; Ramirez-Villegas, J. Predictability of seasonal precipitation across major crop growing areas in Colombia. *Clim. Serv.* **2018**, *12*, 36–47. [[CrossRef](#)]
30. Hossain, M.Z.; Azad, M.A.K.; Karmakar, S.; Mondal, M.N.I.; Das, M.; Rahman, M.M.; Haque, M.A. Assessment of Better Prediction of Seasonal Rainfall by Climate Predictability Tool Using Global Sea Surface Temperature in Bangladesh. *Asian J. Adv. Res. Rep.* **2019**, *4*, 1–13. [[CrossRef](#)]
31. Barnston, A.G.; Tippet, M.K. Do Statistical Pattern Corrections Improve Seasonal Climate Predictions in the North American Multimodel Ensemble Models? *J. Clim.* **2017**, *30*, 8335–8355. [[CrossRef](#)]
32. Horel, J.D. A Rotated Principal Component Analysis of the Interannual Variability of the Northern Hemisphere 500 mb Height Field. *Mon. Weather Rev.* **1981**, *109*, 2080–2092. [[CrossRef](#)]
33. Kirtman, B.P.; Min, D.; Infanti, J.M.; Kinter, J.L.; Paolino, D.A.; Zhang, Q.; Van Den Dool, H.; Saha, S.; Mendez, M.P.; Becker, E.; et al. The North American multimodel ensemble: Phase-1 seasonal-to-interannual prediction; phase-2 toward developing intraseasonal prediction. *Bull. Am. Meteorol. Soc.* **2014**, *95*, 585–601. [[CrossRef](#)]
34. Wang, Q.J.; Shao, Y.; Song, Y.; Schepen, A.; Robertson, D.E.; Ryu, D.; Pappenberger, F. An evaluation of ECMWF SEAS5 seasonal climate forecasts for Australia using a new forecast calibration algorithm. *Environ. Model. Softw.* **2019**, *122*, 104550. [[CrossRef](#)]
35. Araújo, M.L.S.; Sano, E.E.; Bolfe, E.L.; Santos, J.R.N.; dos Santos, J.S.; Silva, F.B. Spatiotemporal dynamics of soybean crop in the Matopiba region, Brazil (1990–2015). *Land Use Policy* **2019**, *80*, 57–67. [[CrossRef](#)]
36. Lima, C.H.R.; Kwon, H.-H.; Kim, H.J. Sparse Canonical Correlation Analysis Postprocessing Algorithms for GCM Daily Rainfall Forecasts. *J. Hydrometeorol.* **2022**, *23*, 1705–1718. [[CrossRef](#)]
37. Salvador, M.A.; Brito, J.I.B. Trend of annual temperature and frequency of extreme events in the MATOPIBA region of Brazil. *Theor. Appl. Climatol.* **2018**, *133*, 253–261. [[CrossRef](#)]
38. dos Reis, L.C.; Silva, C.M.S.; Bezerra, B.G.; Mutti, P.R.; Spyrides, M.H.C.; da Silva, P.E. Analysis of Climate Extreme Indices in the MATOPIBA Region, Brazil. *Pure Appl. Geophys.* **2020**, *177*, 1. [[CrossRef](#)]

39. Assad, E.D.; Marin, F.R.; Pinto, H.S.; Zullo Júnior, J. Mudanças climáticas e agricultura: Uma abordagem agroclimatológica. *Ciência Ambiente* **2007**, *34*, 169–182.
40. Pereira, C.N.; Castro, C.N.D.; Porcionato, G.L. Expansão da agricultura no MATOPIBA e impactos na infraestrutura regional. *Rev. Econ. Agrícola* **2018**, *65*, 15–33. [[CrossRef](#)]
41. Utida, G.; Cruz, F.W.; Etourneau, J.; Bouloubassi, J.; Schefuß, E.; Vuille, M.; Novello, V.F.; Prado, L.F.; Sifeddine, A.; Klein, V.; et al. Tropical South Atlantic influence on Northeastern Brazil precipitation and ITCZ displacement during the past 2300 years. *Sci. Rep.* **2019**, *9*, 1698. [[CrossRef](#)] [[PubMed](#)]
42. Marengo, J.A.; Alves, L.M.; Alvala, R.C.C.; Cunha, A.P.M.A.; Brito, S.B.; Moraes, O.L.L. Climatic characteristics of the 2010–2016 drought in the semiarid Northeast Brazil region. *An. Acad. Bras. Ciências* **2018**, *90*, 1973–1985. [[CrossRef](#)]
43. Pezzi, L.P.; Quadro, M.F.L.; Souza, E.B.; Miller, A.J.; Rao, V.B.; Rosa, E.B.; Santini, M.F.; Bender, A.; Souza, R.B.; Cabrera, M.J.; et al. Oceanic SACZ produces an abnormally wet 2021/2022 rainy season in South America. *Sci. Rep.* **2023**, *13*, 1455. [[CrossRef](#)] [[PubMed](#)]
44. de Moraes, M.D.C.; Gan, M.A.G.; Yoshida, M.C. Features of the upper tropospheric cyclonic vortices of Northeast Brazil in life cycle stages. *Int. J. Climatol.* **2021**, *41*, E39–E58. [[CrossRef](#)]
45. Carvalho, M.A.V.; Oyama, M.D. Variabilidade da largura e intensidade da Zona de Convergência Intertropical Atlântica: Aspectos observacionais. *Rev. Bras. Meteorol.* **2013**, *28*, 305–316. [[CrossRef](#)]
46. Gomes, H.B.; Ambrizzi, T.; Da Silva, B.F.P.; Hodges, K.; Dias, P.L.S.; Herdies, D.; Silva, M.C.L.; Gomes, H.B. Climatology of easterly wave disturbances over the tropical South Atlantic. *Clim. Dyn.* **2019**, *53*, 1393–1411. [[CrossRef](#)]
47. Veber, M.E.; Fedorova, N.; Levit, V. Desenvolvimento de Atividades Convectivas Sobre a Região Nordeste do Brasil, Organizada Pela Extremidade Frontal. *Rev. Bras. Meteorol.* **2020**, *35*, 995–1003. [[CrossRef](#)]
48. Lyra, M.J.A.; Fedorova, N.; Levit, V. Mesoscale convective complexes over northeastern Brazil. *J. S. Am. Earth Sci.* **2022**, *118*, 103911. [[CrossRef](#)]
49. Gonzalez, R.A.; Andreoli, R.V.; Candido, L.A.; Kayano, M.T.; Souza, R.A.F. A influência do evento El Niño—Oscilação Sul e Atlântico Equatorial na precipitação sobre as regiões norte e nordeste da América do Sul. *Acta Amaz.* **2013**, *43*, 469–480.
50. Alves, J.M.; Repelli, C.A. A variabilidade pluviométrica no setor norte do nordeste e os eventos El Niño-Oscilação Sul (ENOS). *Rev. Bras. Meteorol.* **1992**, *7*, 583–592.
51. Martins, E.S.P.R.; Coelho, C.A.S.; Haarsma, R.; Otto, F.E.L.; King, A.D.; Van Oldenborgh, G.J.; Kew, S.; Philip, S.; Júnior, F.C.V.; Cullen, H. A multimethod attribution analysis of the prolonged northeast Brazil hydrometeorological drought (2012–16). *Bull. Am. Meteorol. Soc.* **2018**, *99*, 65–69. [[CrossRef](#)]
52. Kouadio, Y.K.; Servain, J.; Machado, L.A.T.; Lentini, C.A.D. Heavy Rainfall Episodes in the Eastern Northeast Brazil Linked to Large-Scale Ocean-Atmosphere Conditions in the Tropical Atlantic. *Adv. Meteorol.* **2012**, *2012*, 369567. [[CrossRef](#)]
53. Marin, F.; Nassif, D.S.P. Mudanças climáticas e a cana-de-açúcar no Brasil: Fisiologia, conjuntura e cenário futuro. *Rev. Bras. Eng. Agrícola E Ambient.* **2013**, *17*, 232–239. [[CrossRef](#)]
54. da Silva, D.S.; de Moura, F.R.; Santos e Silva, M.A.; da Silva, A.A.G. Spatial Effect Assessment on Maize Production in the Sergipe’s Backwoods. *Braz. J. Dev.* **2019**, *5*, 20677–20701.
55. Barros, G.V.P.; Gomes, H.B.; Nascimento, P.S.R.; Pinto, D.D.C.; Silva, F.D.S.; Costa, R.L. Comparative Analysis of Potential Soil Degradation in the State of Sergipe. *GEO UERJ* **2023**, *42*, e65942.
56. Silva, E.H.d.L.; Silva, F.D.d.S.; Junior, R.S.d.S.; Pinto, D.D.C.; Costa, R.L.; Gomes, H.B.; Júnior, J.B.C.; de Freitas, I.G.F.; Herdies, D.L. Performance Assessment of Different Precipitation Databases (Gridded Analyses and Reanalyses) for the New Brazilian Agricultural Frontier: SEALBA. *Water* **2022**, *14*, 1473. [[CrossRef](#)]
57. Santiago, D.B.; Barbosa, H.A.; Correia Filho, W.L.F.; Oliveira-Júnior, J.F. Interactions of Environmental Variables and Water Use Efficiency in the Matopiba Region via Multivariate Analysis. *Sustainability* **2022**, *14*, 8758. [[CrossRef](#)]
58. Matsunaga, W.K.; Sales, E.S.G.; Assis Júnior, G.C.; Silva, M.T.; Lacerda, F.F.; de Paiva Lima, E.; dos Santos, C.A.C.; de Brito, J.I.B. Application of ERA5-Land reanalysis data in zoning of climate risk for corn in the state of Bahia-Brazil. *Theor. Appl. Climatol.* **2024**, *155*, 945–963. [[CrossRef](#)]
59. Philander, S.G.H.; Gu, D.; Halpern, D.; Lambert, G.; Lau, N.C.; Li, T.; Pacanowski, R.C. Why the ITCZ is mostly North of the Equator. *J. Clim.* **1996**, *9*, 2958–2972. [[CrossRef](#)]
60. Trenberth, K.E. The Definition of El Niño. *Bull. Am. Meteorol. Soc.* **1997**, *78*, 2771–2777. [[CrossRef](#)]
61. Moura, A.D.; Shukla, J. On the dynamics of droughts in northeast Brazil: Observations, theory and numerical experiments with a general circulation model. *J. Atmos. Sci.* **1981**, *38*, 2653–2675. [[CrossRef](#)]
62. Nobre, P.; Shukla, J. Variations of Sea Surface Temperature, Wind Stress, and Rainfall over the Tropical Atlantic and South American. *J. Clim.* **1996**, *9*, 2464–2479. [[CrossRef](#)]
63. Huang, B.; Thorne, P.T.; Banzon, V.F.; Boyer, T.; Chepurin, G.; Lawrimore, J.H.; Menne, M.J.; Smith, T.M.; Vose, R.S.; Zhang, H.-M. Extended Reconstructed Sea Surface Temperature, Version 5 (ERSSTv5): Upgrades, Validations, and Intercomparisons. *J. Clim.* **2017**, *30*, 8179–8205. [[CrossRef](#)]
64. Enfield, D.B.; Alfaro, E.J. The Dependence of Caribbean Rainfall on the Interaction of the Tropical Atlantic and Pacific Oceans. *J. Clim.* **1999**, *12*, 2093–2103. [[CrossRef](#)]

-
65. Servain, J.; Clauzet, G.; Wainer, I.C. Modes of tropical Atlantic climate variability observed by PIRATA. *Geophys. Res. Lett.* **2003**, *30*, 8003. [[CrossRef](#)]
 66. Alves, J.M.B.; Servain, J.; Campos, J.N.B. Relationship between ocean climatic variability and rain-fed agriculture in northeast Brazil. *Clim. Res.* **2009**, *38*, 225–236. [[CrossRef](#)]

Disclaimer/Publisher’s Note: The statements, opinions and data contained in all publications are solely those of the individual author(s) and contributor(s) and not of MDPI and/or the editor(s). MDPI and/or the editor(s) disclaim responsibility for any injury to people or property resulting from any ideas, methods, instructions or products referred to in the content.